Electrochimica Acta 545 (2026) 147758

Contents lists available at ScienceDirect

Electrochimica Acta

journal homepage: www.journals.elsevier.com/electrochimica-acta

Modeling electrochemical impedance spectroscopy of hydrogen complexes during hydrogen evolution on single-atom electrocatalysts

Matteo Spotti [a,1], Nicolò Pianta [a,1], Doriano Brogioli [b], Fabio La Mantia [*,b,c], Giovanni Di Liberto [*,a]

[a] Università degli Studi di Milano – Bicocca, Dipartimento di Scienza dei Materiali, Via Roberto Cozzi 55, 20125 Milano, Italy
[b] Universität Bremen, Energiespeicher- und Energiewandlersysteme, Bibliothekstr. 1, Bremen 28359, Germany
[c] Fraunhofer Institute for Manufacturing Technology and Advanced Material-IFAM, Wiener Str. 12, Bremen 28359, Germany

ARTICLE INFO

Keywords:
SACs
HER
EIS
DFT

ABSTRACT

Single Atom Catalysts (SACs) are an emerging frontier in heterogeneous electrocatalysis. They are made of metal atoms atomically dispersed on a matrix. A lot of attention has been dedicated to the study of Hydrogen Evolution Reaction (HER) mechanism, due to its relevance in energy conversion technologies, both with computational and experimental methods. The classical HER mechanism can be described by a Volmer–Heyrovsky–Tafel mechanism, where the two desorption steps are competitive. The Volmer-Heyrovsky mechanism is conventionally proposed for single-atom catalysts. It has been computationally demonstrated that hydrogen complexes can form on SACs due to their analogy with homogeneous catalysts. Unfortunately, it is hard to "visualize" these species experimentally. Electrochemical Impedance Spectroscopy (EIS) could be the most promising approach to study electrocatalytic mechanisms. In this work, we present microkinetic and Electrochemical Impedance Spectroscopy models for HER on SACs, describing Volmer-Heyrovsky and a mechanism mediated by the formation of hydrogen complexes. Our simulated data, applied to a case study based on Pd@TiN, show that Tafel plots will not suffice in the visualization of hydrogen complexes formation and will need the support of electrochemical impedance spectra in order to clarify the correct mechanism.

1. Introduction

The need for energy transition is triggering current research toward more sustainable chemical processes [1]. A major role is played by catalysis. In this context, electrocatalysis could play a prominent role in the electrification of the chemical industrial sector, given the possibility to use energy produced from renewable sources to power processes at room temperature [2,3]. Hydrogen Evolution Reaction (HER) is one of the most studied reactions, due to its important role in processes such as water splitting and green hydrogen production [4–9]. In this context, one of the major challenges is related to the fact that the catalysis of the HER reaction has always been carried out essentially through the use of expensive and rare elements, such as the Platinum Group Metals (PGMs). This challenge has been addressed over the years by following various strategies, such as the development of PGM-free electrocatalysts [10] or Single-Atom Catalysts (SACs) [11–14]. A SAC is made by single transition metal atoms embedded in a solid supporting matrix, which allows to maximize the efficiency of metal atom use, which is critical when expensive PGMs are considered [15].

One key aspect is that SACs bridge the traditional domains of homogeneous and heterogeneous catalysis, due to their reminiscence of coordination chemistry [16–18]. This has dramatic implications, as reactions could involve intermediates that are unexpected on traditional heterogenous surfaces. In the case of HER, it has been suggested that adsorbed hydrogen complexes (H_2*) could form during the reaction, besides the classical intermediate made by an adsorbed hydrogen atom (H*) [19–23]. This implies the need to go beyond the classical description of the catalytic activity relying on H* only [24].

One open question is to find a way to track these species during the reaction, in order to better understand their role in the reaction mechanism.

The state-of-the-art electrochemical approach to access mechanistic

The manuscript was written through contributions of all authors.

* Corresponding authors.
E-mail addresses: lamantia@uni-bremen.de (F. La Mantia), giovanni.diliberto@unimib.it (G. Di Liberto).

[1] MS and NP equally contributed to this work.

https://doi.org/10.1016/j.electacta.2025.147758
Received 4 September 2025; Received in revised form 20 October 2025; Accepted 8 November 2025
Available online 10 November 2025

information is the analysis of the relation between the applied potential and measured current, which is typically referred as Tafel analysis [25–28]. Another type of analysis that have historically being performed in parallel is Electrochemical Impedance Spectroscopy (EIS) [29], which has the advantage of being able to decouple various processes based on their lifetimes and action times [30–36]. An interesting evolution of the EIS is the so-called dynamic Electrochemical Impedance Spectroscopy [37–40], which allows the collection of information, in the form of impedance spectra, even outside the normal stationarity conditions, which is instead necessary in classical impedance [41]. This translates into the possibility of exploiting large amount of impedance data in a broad range of frequencies and polarization potentials in order to evaluate mechanistic information *operando*.

In the context of theory and simulation, the modeling of Tafel slope is the staple strategy, while simulating impedance spectra under different potential and reaction conditions is a route much less explored, and potentially very effective, given the plethora of information that can be validated or extracted with EIS experiments.

In this work, we assessed the power of combining simulated Tafel analysis and EIS in tracking and detecting hydrogen complexes during Hydrogen Evolution on SACs, with theoretical models. To do so, we considered a model system SAC for hydrogen evolution already studied by some of us [42,43], which is based on Pd atoms embedded in Titanium Nitride (TiN), an emerging supporting matrix for SACs [44,45]. Results suggest that simulated Tafel plots are scarcely effective in tracking hydrogen complexes on SACs. Interestingly, the presence of hydrogen complexes has direct and sizeable effects on the simulated impedance profile, indicating that the formation of hydrogen complexes on SACs can be assessed with EIS.

2. Theoretical approach

2.1. Modeling Tafel plots

The proposed mechanism of Hydrogen Evolution is the Volmer-Heyrovsky-Tafel mechanism. The mechanism involves a first electrochemical hydrogen adsorption (Volmer), followed by two competitive molecular hydrogen desorption steps: one electrochemical (Heyrovsky) and one chemical (Tafel). In acidic conditions the generalized mechanism can be written as:

$$H^+ + e^- + * \rightleftharpoons H^* \quad Volmer \tag{2.1.1}$$

$$H^* + H^+ + e^- \rightleftharpoons H_2 + * \quad Heyrovsky \tag{2.1.2}$$

$$H^* + H^* \rightleftharpoons H_2 + * \quad Tafel \tag{2.1.3}$$

where * represents the catalyst's active site (in the case of SACs, this is the metal atom). Due to the atomic dispersion of the active metal sites in single-atom catalysts, we can assume HER to proceed exclusively via the Volmer–Heyrovsky mechanism [46,47].

The Volmer–Heyrovsky mechanism consists of the following elementary steps:

$$\mathrm{H^+ + e^- + *} \underset{k_1^-}{\overset{k_1^+}{\rightleftharpoons}} \mathrm{H^*} \tag{2.1.4}$$

$$\mathrm{H^* + H^+ + e^-} \underset{k_2^-}{\overset{k_2^+}{\rightleftharpoons}} \mathrm{H_2 + *} \tag{2.1.5}$$

where $k_i^+ = k_i^{+,0} e^{-\frac{\beta F\phi}{RT}}$, $k_i^- = k_i^{-,0} e^{\frac{(1-\beta)F\phi}{RT}}$ are the forward and backward kinetic constants for the *i th* step, respectively.

We here define θ_{H^*} as the coverage of H* intermediate adsorbed on the catalyst, N the moles of active sites per unit of area, c_{H^+} the concentration of H^+ and c_{H_2} the concentration of H_2 at electrode surface. We also assume β, the symmetry factor, always equal to 0.5.

Assuming steady-state approximation, the coverage of adsorbed hydrogen (H*) remains constant: $\frac{d\theta_{H^*}}{dt} = 0$. As a result, the Volmer and Heyrovsky rates are equal, and the overall rate of the reaction can be expressed as either $r_{overall} = r_1 = r_2$. (The detailed derivation is reported in Appendix A.1). Then, Faradaic current density can be written as:

$$i_F = -2Fr_{overall} = -2F\left[k_1^+ c_{H^+} N \frac{k_1^- + k_2^+ c_{H^+}}{k_1^+ c_{H^+} + k_1^- + k_2^+ c_{H^+} + k_2^- c_{H_2}} - k_1^- N \frac{k_1^+ c_{H^+} + k_2^- c_{H_2}}{k_1^+ c_{H^+} + k_1^- + k_2^+ c_{H^+} + k_2^- c_{H_2}}\right] \tag{2.1.6}$$

The mechanism passing through the formation of hydrogen complexes in SAC consists of the elementary steps expressed in (2.1.4) and in a modified version of (2.1.5), with the addition of a third final step:

$$\mathrm{H^* + H^+ + e^-} \underset{k_2^-}{\overset{k_2^+}{\rightleftharpoons}} \mathrm{H_2^*} \tag{2.1.7}$$

$$\mathrm{H_2^*} \underset{k_3^-}{\overset{k_3^+}{\rightleftharpoons}} \mathrm{H_2 + *} \tag{2.1.8}$$

where $k_3^+ = k_3^{+,0}$ and $k_3^- = k_3^{-,0}$ are the forward and backward kinetic constants of the chemical desorption step of molecular hydrogen.

In the molecular hydrogen Volmer-Heyrovsky mechanism there are two intermediates: H* and H_2*. Then, steady-state assumption imposes: $\frac{d\theta_{H^*}}{dt} = 0$ and $\frac{d\theta_{H_2^*}}{dt} = 0$. These intermediates influence the net Faradaic current by occupying active sites and enabling back-reactions. Their contributions are implicitly considered in the analytical expression of the Faradaic density current (a.2.12), Appendix A.2.

To better describe the physical chemistry of the process it is important to add diffusion correction to our models. This involves calculating the steady-state concentrations of H^+ (c_{H^+}) and H_2 (c_{H_2}) at the electrode surface. We adopt a finite diffusion approximation, which assumes that the concentration gradient is confined to a thin boundary layer, and beyond this region, the bulk concentration remains constant. In the context of a Rotating Disk Electrode (RDE), this approximation is particularly valid due to the well-defined hydrodynamic conditions it creates. In fact, the rotation of the disk establishes a thin, steady-state diffusion layer near the electrode surface [48]. Inside this layer, mass transport is dominated by diffusion, while convective transport governs the bulk solution outside.

We use a self-consistent approach based on the Levich equation to estimate the surface concentration of reactants under these conditions. Levich equation allows to linearly correlate the Faradaic current with c_{H^+} at electrode surface:

$$i_F(c_{H^+}) = 0.0620 n F D_H^{\frac{2}{3}} \Omega^{\frac{1}{2}} \nu^{-\frac{1}{6}} \left(c_{H^+} - c_{H^+}^{bulk}\right) \tag{2.1.9}$$

Where n is the number of electrons involved in the reaction, Ω is the rotation rate, ν is the kinematic viscosity, $c_{H^+}^{bulk}$ is the reactant concentration in bulk and c_{H^+} is the reactant concentration at electrode surface. A correction factor of 0.1 is applied to the constant with a value of 0.620 to obtain the Faradaic density current expressed in A cm^{-2}. To simplify the model, we solved the Levich equation only for c_{H^+}. The change in

concentration of H_2 near the electrode surface has been taken into account by applying the thermodynamic consistency:

$$c_{H_2} = c_{H^+}^2 \exp\left(-\frac{nF\phi}{RT}\right) \tag{2.1.10}$$

A detailed discussion is reported in Appendix A.3

2.2. Modeling EIS

Electrochemical Faradaic admittance, $Y_F = 1/Z_F$ (where Z_F is Faradaic impedance), is defined as the ratio between the frequency-dependent current density perturbation (the phasor of i_F, $\widetilde{i_F}$) and the frequency-dependent applied potential perturbation (the phasor of ϕ, $\widetilde{\phi}$). For the Volmer–Heyrovsky mechanism without diffusion, i_F depends on both the polarization potential ϕ and the adsorbed hydrogen coverage θ_{H^*}.

By applying a first-order Taylor series expansion of current density with respect to steady-state and assuming sinusoidal perturbations, we obtain the following expression for Faradaic admittance:

$$\frac{1}{Z_F} = \frac{\widetilde{i_F}}{\widetilde{\phi}} = \left(\frac{\partial i_F}{\partial \phi}\right)_{\theta^*_{H^*}} + \left(\frac{\partial i_F}{\partial \theta_{H^*}}\right)_{\phi^*} \frac{\widetilde{\theta}_{H^*}}{\widetilde{\phi}} \tag{2.2.1}$$

$\frac{\widetilde{\theta}_{H^*}}{\widetilde{\phi}}$ is the only unknown term of (2.2.1) and can be derived through dynamic equations governing the coverage, leading to:

$$\frac{\widetilde{\theta}_{H^*}}{\widetilde{\phi}} = \frac{\left(\frac{\partial g}{\partial \phi}\right)_{\theta^*_{H^*}}}{j\omega - \left(\frac{\partial g}{\partial \theta_{H^*}}\right)_{\phi^*}} \tag{2.2.2}$$

Substituting (2.2.2) into (2.2.1), it is possible to write the expression of Faradaic admittance for Volmer-Heyrovsky mechanism in the absence of diffusion correction. (The complete derivation is reported in Appendix B.1).

$$\frac{1}{Z_F} = \left(\frac{\partial i_F}{\partial \phi}\right)_{\theta^*_{H^*}} + \left(\frac{\partial i_F}{\partial \theta_{H^*}}\right)_{\phi^*} \frac{\left(\frac{\partial g}{\partial \phi}\right)_{\theta^*_{H^*}}}{j\omega - \left(\frac{\partial g}{\partial \theta_{H^*}}\right)_{\phi^*}} \tag{2.2.3}$$

To account for diffusion of H^+ and H_2, additional terms are introduced in the current expression, now depending also on concentrations: $i_F = i_F(\phi, \theta_{H^*}, c_{H^+}, c_{H_2})$. The resulting admittance is:

$$\frac{1}{Z_F} = \left(\frac{\partial i_F}{\partial \phi}\right)_{\theta^*_{H^*}, c^*_{H^+}, c^*_H 2} + \left(\frac{\partial i_F}{\partial \theta_{H^*}}\right)_{\phi^*, c^*_{H^+}, c^*_H 2} \frac{\widetilde{\theta}_{H^*}}{\widetilde{\phi}} + \left(\frac{\partial i_F}{\partial c_{H^+}}\right)_{\phi^*, \theta^*_{H^*}, c^*_H 2} \frac{\widetilde{c}_{H^+}}{\widetilde{\phi}} + \left(\frac{\partial i_F}{\partial c_{H_2}}\right)_{\phi^*, \theta^*_{H^*}, c^*_{H^+}} \frac{\widetilde{c}_{H_2}}{\widetilde{\phi}} \tag{2.2.4}$$

Unknown terms $\frac{\widetilde{\theta}_{H^*}}{\widetilde{\phi}}$, $\frac{\widetilde{c}_{H^+}}{\widetilde{\phi}}$ and $\frac{\widetilde{c}_{H_2}}{\widetilde{\phi}}$ can be evaluated solving a coupled linear system derived from Fick's laws and kinetic rate expressions. The complete derivation is reported in Appendix B.4.

It is important to underline that approximating the diffusion mechanism as semi-infinite is valid as long as the penetration depth of the periodic perturbation (i.e., spatial region perturbated by the ac current used in the EIS experiment) is much smaller than the diffusion layer. This translates in a limit frequency, as in (b.3.4), above which semi-infinite diffusion is seen. Under most conditions (like those applied for the simulations performed in this work), such threshold is low enough to allow almost all the information to be extracted from the impedance spectra. A detailed discussion of this approximation and its applicability is proposed in Appendix B.3.

When we move to the Volmer-Heyrovsky mechanism with hydrogen complexes, the dependencies of density current are different than the conventional case: $i_F = i_F\left(\phi, \theta_{H^*}, \theta_{H_2^*}, c_{H^+}\right)$. Following an analogous approach, the admittance becomes:

$$\frac{1}{Z_F} = \left(\frac{\partial i_F}{\partial \phi}\right)_{\theta^*_{H^*}, \theta^*_{H_2^*}, c^*_{H^+}} + \left(\frac{\partial i_F}{\partial \theta_{H^*}}\right)_{\phi^*, \theta^*_{H_2^*}, c^*_{H^+}} \frac{\widetilde{\theta}_{H^*}}{\widetilde{\phi}} + \left(\frac{\partial i_F}{\partial \theta_{H_2^*}}\right)_{\phi^*, \theta^*_{H^*}, c^*_{H^+}} \frac{\widetilde{\theta}_{H_2^*}}{\widetilde{\phi}} + \left(\frac{\partial i_F}{\partial c_{H^+}}\right)_{\phi^*, \theta^*_{H^*}, \theta^*_{H_2^*}} \frac{\widetilde{c}_{H^+}}{\widetilde{\phi}} \tag{2.2.5}$$

Unknown terms $\frac{\widetilde{\theta}_{H^*}}{\widetilde{\phi}}$, $\frac{\widetilde{\theta}_{H_2^*}}{\widetilde{\phi}}$ and $\frac{\widetilde{c}_{H^+}}{\widetilde{\phi}}$ can again be determined by solving an appropriate system of equations. The complete derivation is reported in Appendix B.2 and B.5.

For both models, the presence of the electrochemical double layer must be considered in the impedance equation; it is modeled as a capacitor with a constant capacitance, C_{dl}.

$$Z = \frac{Z_F}{1 + j\omega C_{dl} Z_F} \tag{2.2.6}$$

In Table 1 are reported the values of simulation parameters needed for numerical resolution of both microkinetic and EIS models.

It has been experimentally and theoretically demonstrated that the supporting electrolyte, in particular its cation, can have significant effects on the kinetics of the HER reaction, [49–51] and is also known to have an effect on impedance., [52,53] To simplify our model, we decided to simulate our impedance using a high concentration of H^+ (1 M), so as not to have the need to include the supporting electrolyte in the calculations, which is outside of the scope of this first model. The inclusion of the role of supporting electrolyte will be considered in a future dedicated study.

Table 1
Simulation parameters adopted for the numerical simulation of microkinetic and EIS models.

Parameter	Simulation value
N/mol cm^{-2}	10^{-9}
β	0.5
T/K	298
$c^{bulk}_{H^+}$/mol L^{-1}	1
$c^{bulk}_{H_2}$/mol L^{-1}	1
ω/rad s^{-1}	1 - 10^6
C_{dl}/μF cm^{-2}	20
D_{H^+}/m^2 s^{-1}	$9.31{\cdot}10^{-9}$
D_{H_2}/m^2 s^{-1}	$4.50{\cdot}10^{-9}$
Ω/rpm	1000
ν/m^2 s^{-1}	10^{-6}

2.3. Computational details

Both Tafel plots, as well as impedance spectra as a function of frequency and electrode polarization, are strongly affected by both thermodynamics and kinetics of all reaction steps, as evident from Sections 2.1 and 2.2. In order to minimize the number of arbitrary parameters, the thermodynamics of the reaction steps 2.1.4, 2.1.5 and 2.1.8 was obtained from DFT calculations performed on the Pd@TiN system. Spin-polarized Density Functional Theory (DFT) calculations were performed using the VASP package [54–56] The Perdew-Burke-Ernzerhof (PBE) parametrization was employed for the exchange-correlation functional [57]. Projector Augmented Wave (PAW) pseudopotentials were used to describe core electrons [58,59], and valence electrons were expanded with a plane wave, using a kinetic energy cutoff of 400 eV. Electronic structure optimizations were considered converged after achieving a threshold criterion of 10^{-5} eV between different steps. The DFT + U approach was used to tame the self-interaction error of pure GGA

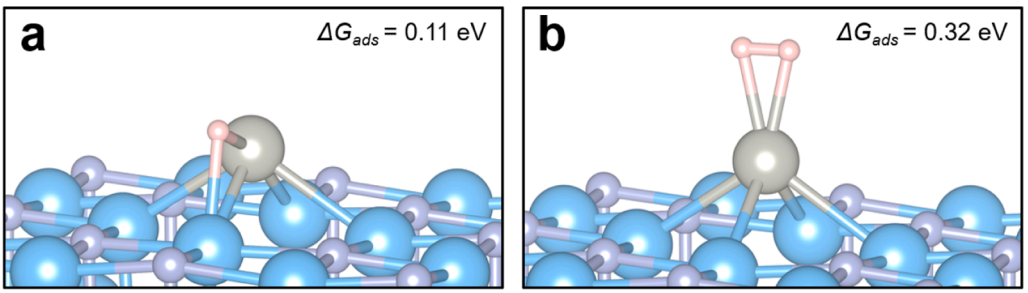

Fig. 1. Adsorption configurations of H* (panel a) and H_2* (panel b) on Pd@TiN.

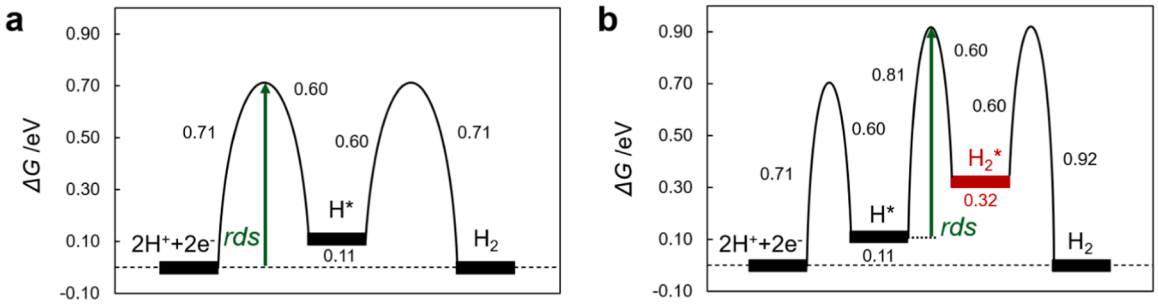

Fig. 2. Gibbs free energy profile for conventional volmer-heyrovsky mechanism (panel a) and volmer-heyrovsky mechanism with the formation of hydrogen complex (panel b).

functionals, incorporating a U term of 3.33 eV for Pd atom. The choice of the working U parameter is generally arbitrary. In our case, we used a value taken from a seminal work of Anisimov and co-workers, which has been extensively tested for HER on SACs to approach predictions close to benchmark PBE0 data [60–62]. Geometry optimization convergence criterion was set to 10^{-2} eV·Å^{-1}. Grimme's D3 scheme was used to account for dispersion forces [63]. Reciprocal space was sampled with a 2 × 2 × 1 k-point grid. We started from the experimental cubic bulk crystal structure of TiN and performed full optimization. A five-layer thick low-index (001) surface was modeled from the bulk structure. Then, a 2 × 2 expansion of the primitive cell was considered, yielding lattice parameters of $a = b = 8.384$ Å and $\gamma = 90°$. A Pd atom was introduced in the system in place of a nitrogen vacancy, Pd@TiN, following previous works [42,43]. All the atomic coordinates were fully relaxed. The stability of the reaction intermediates was calculated by adopting the Computational Hydrogen Electrode approach (CHE) [64–66]. The Gibbs free energy was estimated as:

$$\Delta G = \Delta E - T\Delta S + \Delta E_{ZPE}$$

where ΔE is the calculated DFT energy, $T\Delta S$ is the entropic contribution and ΔE_{ZPE} is the zero-point energy correction. $T\Delta S$ of solid-state species was neglected, and that of gas-phase molecules was taken from International Tables. At 298 K, $T\Delta S_{H2}$, is equal to 0.40 eV. We adopted the value 0.04 eV, for the zero-point energy correction [67]. In CHE, any reaction barriers different from those arising from thermochemistry are neglected. In our case, we need to introduce microkinetic model reaction barriers. We assigned to the activation energies the value of 0.6 eV, to achieve an exchange current density for the Volmer–Heyrovsky mechanism comparable to that of platinum electrodes [68,69]. Of course, for better quantitative predictions more elaborated approaches should be adopted [70,71], however this is outside the scope of this work. Starting from the kinetic energy barriers ($\Delta G_i^{\neq}$) we estimate kinetic constants (k_i^0) using Eyring equation from the framework of transition state theory.

$$k_i^0 = \frac{K_B T}{h} e^{-\frac{\Delta G_i^{\neq}}{RT}} \qquad (2.3.1)$$

This leads to a value of i_0 equal to −1.15 mA cm^{-2} for Volmer-Heyrovksy and −0.02 mA cm^{-2} for molecular hydrogen Volmer-Heyrovsky.

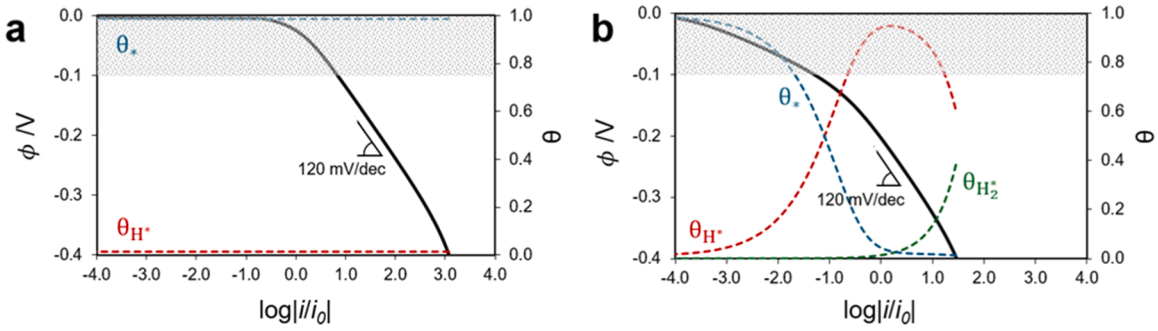

Fig. 3. Simulated Tafel plots for volmer-heyrovsky mechanism (panel a) and molecular hydrogen volmer-heyrovsky mechanism (panel b). The potential range between 0 and −0.1 V vs NHE was not considered because it is not included in the validity region of Tafel regime., [80] The trends of intermediate coverages are shown as colored dashed lines.

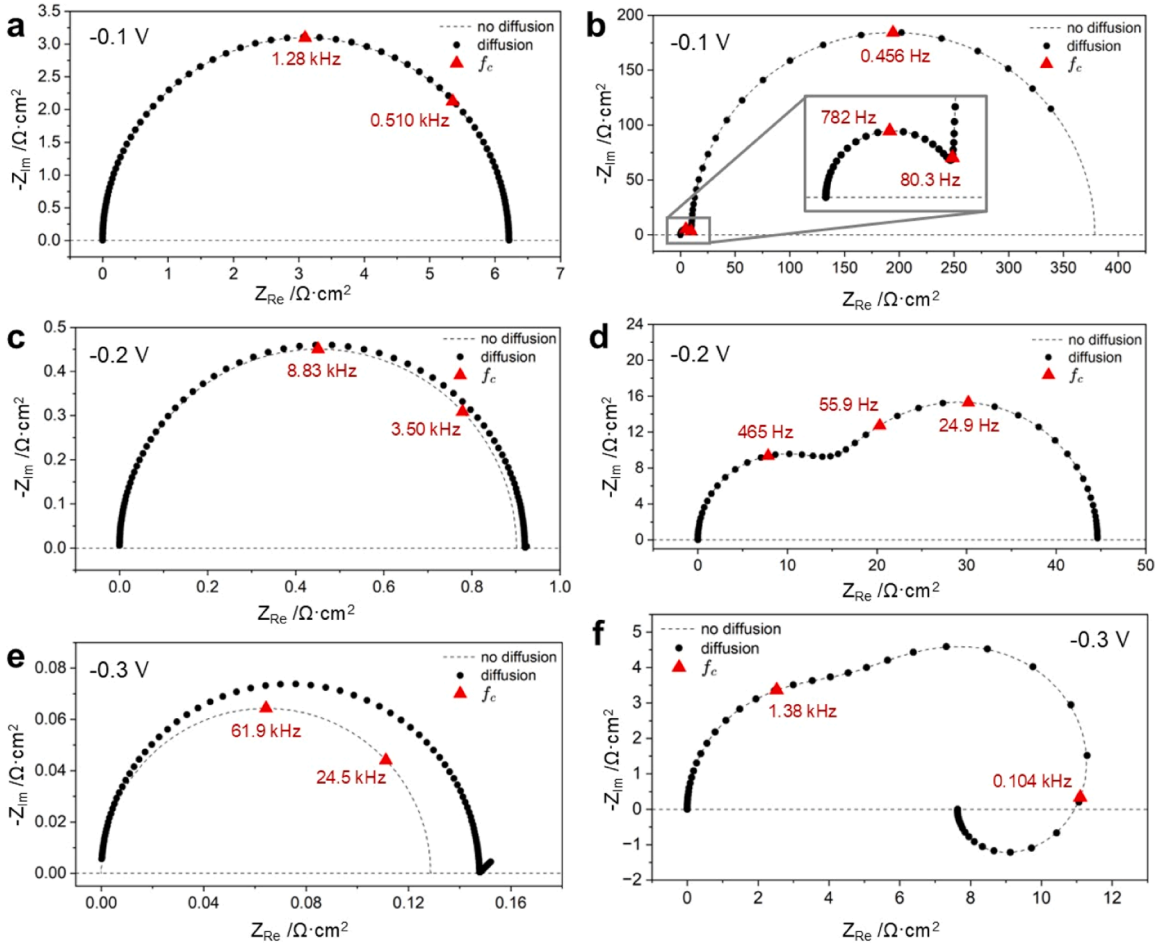

Fig. 4. Simulated Nyquist plots for volmer-heyrovsky mechanism at −0.1 V vs NHE (panel a), −0.2 V vs NHE (panel c), −0.3 V vs NHE (panel e) and molecular hydrogen volmer-heyrovsky mechanism at −0.1 V vs NHE (panel b), −0.2 V vs NHE (panel d), −0.3 V vs NHE (panel f). Characteristic frequencies are determined as the roots of the electrochemical admittance function. The impedance calculated without diffusion is shown as a grey dashed line, while the impedance from the diffusion-corrected model is shown as black dots.

3. Results and discussion

We start with the analysis of the DFT calculations performed on the model system and reaction, which provide the thermodynamic parameters used in the subsequent microkinetic and electrochemical impedance model. The adsorption of H* is nearly thermoneutral with respect to HER reactants and products with calculated Gibbs free energy equal to 0.11 eV, Fig. 1. The calculated Pd-H distance (d_{PdH}) is 1.78 Å. It is also possible to adsorb H* on top of the metal atom, Fig. S1. The resulting structure is slightly less stable, $\Delta G_{H^*} = 0.22$ eV, with a value of $d_{PdH} =$ 1.60 Å. Once H* is formed through adsorption, it is possible to form a hydrogen complex (H_2*) characterized by $d_{PdH} = 1.88$ Å. The H—H distance is slightly elongated (0.80 Å) with respect to the value of isolated H_2, 0.75 Å, in line with the typical values of hydrogen complexes [72–74]. The formation of the complex is slightly endergonic, with $\Delta G_{H2}^* = 0.32$ eV. Table S1 reports calculated distances and free energy. As mentioned above, once determined the thermodynamic reaction profile we assume that reaction barriers 0.6 eV higher than reaction intermediates. This leads to the picture sketched in Fig. 2. It must be underlined that our purpose is not to provide quantitative predictions on a real case but to work on a model system where both H* and H_2* could play a role in the reaction mechanism.

By numerically solving the kinetics derived in the microkinetic modeling, it is possible to simulate the Faradaic current density as a function of the applied potential. The simulated results can be represented as Tafel plots, where the applied potential (ϕ) is plotted against $\log|i/i_0|$, Fig. 3. In the Tafel regime, both the Volmer–Heyrovsky mechanism and the molecular hydrogen Volmer–Heyrovsky mechanism yield slopes of 120 mV/decade. This slope is known to be characteristic of the Volmer step, as well as of the Heyrovsky step under strongly reducing conditions [75,76]. Moreover, it is possible to observe that the value of log|i/i0| in the two cases is different at −0.4 V, Fig. 3a and 3b However, this aspect cannot be used as clear information to distinguish between the two proposed mechanisms, as it directly depends by the DFT calculated Gibbs free adsorption energy of intermediates. Since DFT calculations are known to have limited quantitative accuracy, adsorption energies should be treated with caution [77,78]. Consequently, any exchange current density calculated from such parameters cannot have quantitative agreement with experiments [79]. Then, Tafel analysis alone does not provide a clear information to distinguish the formation of hydrogen complexes on Pd@TiN. Specifically, there is no significant difference in the Tafel slopes that could serve as a descriptor for hydrogen complex formation.

Simulated EIS spectra in the form of Nyquist plots, calculated at –0.1 V vs NHE and –0.2 V vs NHE, are reported in Fig. 4. Focusing on the Volmer-Heyrovsky mechanism, presented in Fig. 4a-4c for the two potentials, it is possible to always observe a single semicircle at high frequencies, linked to charge transfer processes. In contrast, assuming the molecular hydrogen Volmer-Heyrovsky mechanism already from –0.1 V vs NHE (Fig. 4b) two separate semicircles are visible, one at low frequencies and one at high frequencies. This behavior is even more pronounced at –0.2 V vs NHE (Fig. 4d). It is important to underline that the

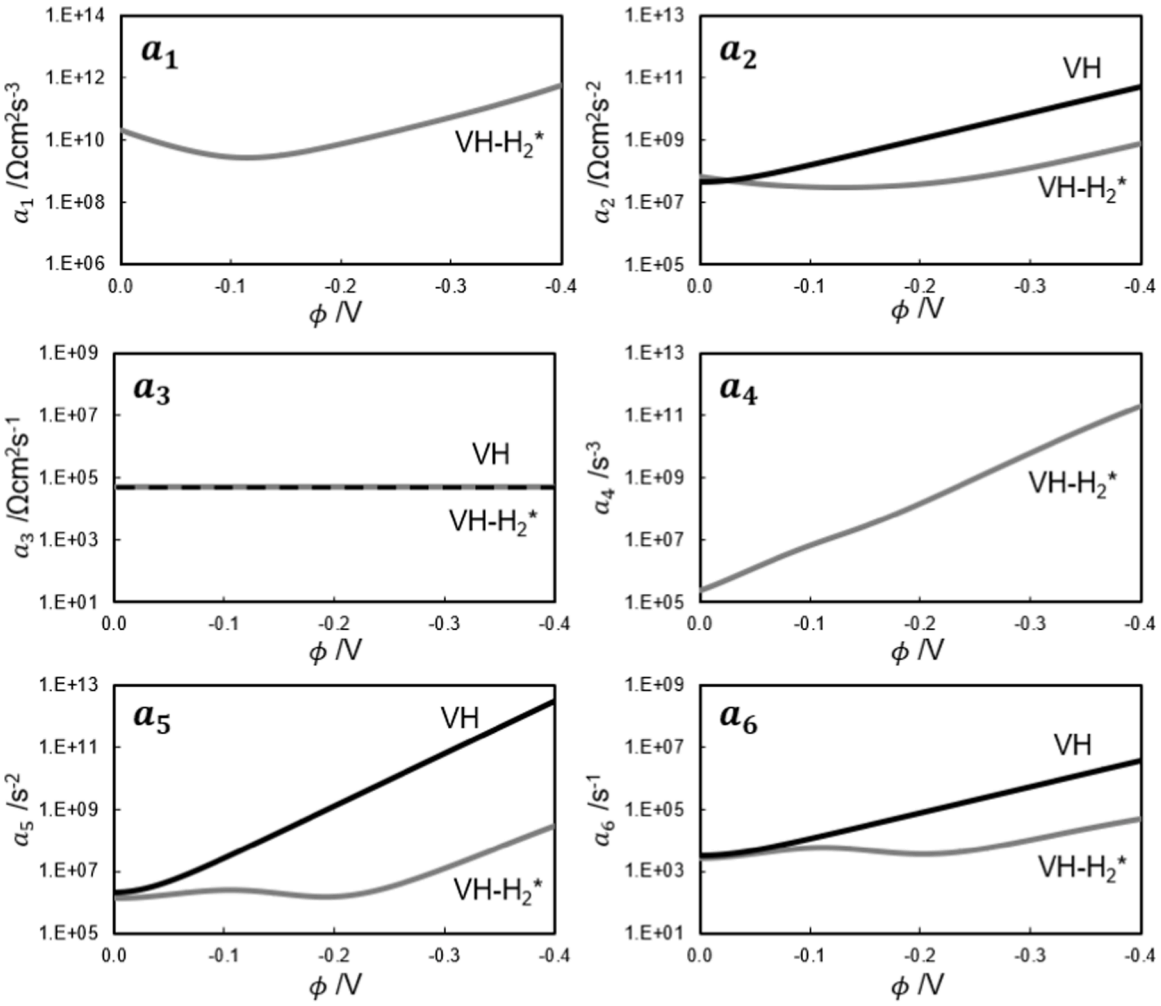

Fig. 5. Simulated EIS parameters for volmer-heyrovsky (black lines) and molecular hydrogen volmer-heyrovsky mechanism (grey lines) with respect to polarization potential.

number of visible semicircles in the impedance spectra is not a universal indicator of a specific reaction mechanism [31,81,82]. Nevertheless, the qualitative difference in the spectra provides a positive indication of the possible detection of hydrogen complexes by properly fitting experimental data.

When a more reductive polarization potential, such as –0.3 V vs NHE, is applied, the difference between the two simulated impedance spectra, corresponding to the proposed mechanisms, becomes even more pronounced, as seen in Fig. 4e-4f. For the Volmer–Heyrovsky mechanism (Fig. 4e), the spectrum displays a single semicircle, followed by a 45◦ diffusive tail at low frequencies, linked to mass transfer processes at electrode surface. In contrast, when hydrogen complex formation is considered (Fig. 4f), an inductive loop appears at low frequencies. This inductive behavior suggests that a chemical desorption step plays a sizeable role in determining the overall reaction rate [30,83]. Indeed, according to our model reaction profile (Fig. S2), the application of a polarization potential ϕ equal to –0.3 V vs NHE reduces the forward kinetic barrier for the Heyrovsky step forming H_2* from 0.81 eV to 0.66 eV, assuming a dependence of the kinetic barrier according to $\widetilde{\Delta G_f^{\neq}} = \Delta G_f^{\neq} + \beta e\phi$ [84]. More details are reported in Section S1. Therefore, the energy cost to form H_2* becomes comparable to that of molecular hydrogen desorption, 0.60 eV (Fig. S2).

Simulated EIS spectra provide additional insight that may help distinguish between the two proposed mechanisms. Interestingly, the Volmer–Heyrovsky impedance is more affected by diffusion control compared to that of the molecular hydrogen Volmer–Heyrovsky mechanism. In the former case, the diffusion tail becomes more pronounced as the applied potential increases.

These results suggest that it is possible to theoretically detect the formation of hydrogen complexes on SACs during HER using EIS.

In experimental electrochemical impedance spectroscopy, it is possible to fit measured spectra using mathematical models of impedance. A possible approach involves expressing the impedance as the ratio of two polynomials in the complex angular frequency variable. This is an already established approach for representing impedance data, which has been demonstrated to be mathematically equivalent to the most famous equivalent electrical circuit representations [85,86]. Defining $s = j\omega$, for Volmer-Heyrovsky and molecular hydrogen Volmer-Heyrovsky mechanisms it is possible to express electrochemical impedance as:

$$Z_{tot}^{VH} = \frac{a_2 + a_3 s}{a_5 + a_6 s + s^2} \tag{3.1}$$

$$Z_{tot}^{VH-H_2^*} = \frac{a_1 + a_2 s + a_3 s^2}{a_4 + a_5 s + a_6 s^2 + s^3} \tag{3.2}$$

Where the terms a_1, a_2, a_3,... sharing the same subscript in different equations have identical physical units (dimensions).

Comparing (3.1) and (3.2) with full expression of impedance derived from EIS models, it is possible to find the expressions for all a_i parameters (see Appendix B.6). In Fig. 5 all EIS parameters are reported with

respect to polarization potential, divided by their physical dimension. It is interesting to observe that there is a clear difference in trend between the two proposed mechanisms.

4. Conclusions

In this work, we investigated theoretically the possibility to detect the role of hydrogen complexes in HER on Single-Atom Catalysts. We took a model system made of a Pd-based SAC where the support is TiN, and model electrochemical behavior in the form of Tafel curves and impedance spectra at different polarization potentials. The results show how it is not possible to distinguish between the two reaction paths through Tafel analysis. On the other hand, simulated impedance spectra show an important difference between the two reaction paths. The difference between the two systems is further accentuated at very negative polarization potentials, where the presence of H_2* also translates into an inductance loop, probably due to desorption of molecular hydrogen.

These results indicate that EIS has the potential to provide insight into the role of hydrogen complexes in SACs, as the qualitative shape of spectra is sensitive. Indeed, the fitting of models neglecting and accounting for hydrogen complexes to experimental data will help to better understand their role in HER in Single-Atom Catalysis. This is expected to be even more true when classical EIS is substituted by dEIS, as the latter is known to provide a much greater amount of information (i.e., number of spectra per single experiment) than a classical experiment.

To conclude, we would like to propose here to raise a series of aspects relevant to design experiments that can be used in practice to evaluate which of the two mechanisms is dominant in the electrocatalyst under consideration. Since diffusion is never the rate determining step of the molecular hydrogen Volmer-Heyrovsky mechanism, one can simply measure the impedance at different potentials and, most importantly, RDE rotating speed. If the spectra remain unchanged upon rotation speed change, this will mean that H_2* intermediates are present and that their desorption is indeed the rate determining step, otherwise a more common Volmer-Heyrovsky mechanism is probably dominant. Also, a study of the parameters resulting from the fitting of the experimental data with the ratio of polynomials could also be added, as they have different trends in the Volmer-Heyrovsky and molecular hydrogen Volmer-Heyrovsky mechanisms and can be used to detect which model is better suitable to fit the data. Last, one could perform quantum chemical calculation considering and neglecting the formation of H_2*, and use the predicted quantities to predict EIS spectra to be compared with measured ones.

CRediT authorship contribution statement

Matteo Spotti: Writing – review & editing, Methodology, Investigation, Data curation. **Nicolò Pianta:** Writing – review & editing, Methodology, Investigation. **Doriano Brogioli:** Writing – review & editing, Validation, Supervision. **Fabio La Mantia:** Writing – review & editing, Supervision, Methodology. **Giovanni Di Liberto:** Writing – review & editing, Writing – original draft, Supervision, Project administration.

Declaration of competing interest

The authors declare that they have no known competing financial interests or personal relationships that could have appeared to influence the work reported in this paper.

Acknowledgements

We gratefully thank Prof. Gianfranco Pacchioni for useful discussion. Access to the CINECA supercomputing resources was granted via ISCRAB. We also thank the COST Action 18234 supported by COST (European Cooperation in Science and Technology). GDL has received funding through the PRIN project "SACtoH2″ (project code P2022AZETB by the Italian Ministry for Universities and Research (MUR), in the context of the National Recovery and Resilience Plan and co-financed by the European Commission - Next Generation EU (Mission 4, Component 1).

Supplementary materials

Supplementary material associated with this article can be found, in the online version, at doi:10.1016/j.electacta.2025.147758.

Appendix

A. Microkinetic modeling

A.1. Volmer-heyrovsky mechanism

The Volmer–Heyrovsky mechanism consists of the following elementary steps:

$$H^+ + e^- + * \underset{k_1^-}{\overset{k_1^+}{\rightleftharpoons}} H^* \tag{a.1.1}$$

$$H^* + H^+ + e^- \underset{k_2^-}{\overset{k_2^+}{\rightleftharpoons}} H_2 + * \tag{a.1.2}$$

where $k_i^+ = k_i^{+,0} e^{-\frac{\beta F \phi}{RT}}$, $k_i^- = k_i^{-,0} e^{\frac{(1-\beta) F \phi}{RT}}$ are the forward and backward kinetic constants for the i th step, respectively.

We define θ_{H^*} as the coverage of H* intermediate adsorbed on the catalyst, N the moles of active sites per unit of area, c_{H^+} the concentration of H^+ and c_{H_2} the concentration of H_2 at electrode surface. We also assume β, the symmetry factor, always equal to 0.5.

The rate of each step is:

$$r_1 = r_1^+ - r_1^- = k_1^+ c_{H^+} N(1 - \theta_{H^*}) - k_1^- N \theta_{H^*} \tag{a.1.3}$$

$$r_2 = r_2^+ - r_2^- = k_2^+ c_{H^+} N \theta_{H^*} - k_2^- c_{H_2} N(1 - \theta_{H^*}) \tag{a.1.4}$$

The main assumption of the steady-state approximation is that the rate of change in the coverage of intermediates is $\frac{d\theta_{H^*}}{dt} = 0$. If we explicit it, we

obtain:

$$\frac{d\theta_{H^*}}{dt} = \frac{r_1 - r_2}{N} = k_1^+ c_{H^+}(1-\theta_{H^*}) - k_1^- \theta_{H^*} - k_2^+ c_{H^+}\theta_{H^*} + k_2^- c_{H_2}(1-\theta_{H^*}) = 0 \tag{a.1.5}$$

Solving (a.1.5), the following expression of the coverage of adsorbed hydrogen (H*) is obtained:

$$\theta_{H^*} = \frac{k_1^+ c_{H^+} + k_2^- c_{H_2}}{k_1^+ c_{H^+} + k_1^- + k_2^+ c_{H^+} + k_2^- c_{H_2}} \tag{a.1.6}$$

At steady-state conditions, the overall reaction rate can be expressed either as r_1 or r_2, as they are equal. Substituting (a.1.6) in (a.1.3) it is possible to write:

$$r_{overall} = r_1 = k_1^+ c_{H^+} N \frac{k_1^- + k_2^+ c_{H^+}}{k_1^+ c_{H^+} + k_1^- + k_2^+ c_{H^+} + k_2^- c_{H_2}} - k_1^- N \frac{k_1^+ c_{H^+} + k_2^- c_{H_2}}{k_1^+ c_{H^+} + k_1^- + k_2^+ c_{H^+} + k_2^- c_{H_2}} \tag{a.1.7}$$

Finally, the Faradaic current density can be calculated as:

$$i_F = -2Fr_{overall} = -2F\left[k_1^+ c_{H^+} N \frac{k_1^- + k_2^+ c_{H^+}}{k_1^+ c_{H^+} + k_1^- + k_2^+ c_{H^+} + k_2^- c_{H_2}} - k_1^- N \frac{k_1^+ c_{H^+} + k_2^- c_{H_2}}{k_1^+ c_{H^+} + k_1^- + k_2^+ c_{H^+} + k_2^- c_{H_2}}\right] \tag{a.1.8}$$

In Tafel plots it is common to express $\log|i/i_0|$ rather than $\log|i|$, where i_0 is the exchange current density of the electrochemical reaction. The exchange current density describes the rate at which oxidation and reduction reactions occur simultaneously and at the same rate on the surface of the electrode when it is at equilibrium, implying:

$$i_{cathodic} = i_{anodic} = i_0 \tag{a.1.9}$$

An analytical expression of i_0 for hydrogen evolution can be derived by applying the steady-state approximation to the reaction rate at zero polarization potential. For instance, considering the cathodic direction, one can proceed as follows.

$$H^+ + e^- + * \underset{k_1^{0,-}}{\overset{k_1^{0,+}}{\rightleftharpoons}} H^* \tag{a.1.10}$$

$$H^+ + H^* + e^- \underset{k_2^{0,-}}{\overset{k_2^{0,+}}{\rightleftharpoons}} H_2 + * \tag{a.1.11}$$

The rate of each step is:

$$r_{1,0} = r_{1,0}^+ - r_{1,0}^- = k_1^{+,0} c_{H^+} N\left(1-\theta_{H^*,0}\right) - k_1^{-,0} N \theta_{H^*,0} \tag{a.1.12}$$

$$r_{2,0} = r_{2,0}^+ - r_{2,0}^- = k_2^{+,0} c_{H^+} N \theta_{H^*,0} - k_2^{-,0} c_{H_2} N\left(1-\theta_{H^*,0}\right) \tag{a.1.13}$$

Using steady-state assumption, it is possible to find the expression of the coverage:

$$\frac{d\theta_{H^*,0}}{dt} = \frac{r_{1,0} - r_{2,0}}{N} = k_1^{0,+} c_{H^+}\left(1-\theta_{H^*,0}\right) - k_1^{0,-}\theta_{H^*,0} - k_2^{0,+} c_{H^+}\theta_{H^*,0} + k_2^{0,-} c_{H_2}\left(1-\theta_{H^*,0}\right) = 0 \tag{a.1.14}$$

$$\theta_{H^*,0} = \frac{k_1^{0,+} c_{H^+} + k_2^{0,-} c_{H_2}}{k_1^{0,+} c_{H^+} + k_1^{0,-} + k_2^{0,+} c_{H^+} + k_2^{0,-} c_{H_2}} \tag{a.1.15}$$

Finally, it is possible to obtain the expression of the overall rate at zero polarization potential and then the exchange current density.

$$r_{overall,0} = r_{1,0}^+ = k_1^{+,0} c_{H^+} N \frac{k_1^{0,+} c_{H^+} + k_2^{0,-} c_{H_2}}{k_1^{0,+} c_{H^+} + k_1^{0,-} + k_2^{0,+} c_{H^+} + k_2^{0,-} c_{H_2}} \tag{a.1.16}$$

$$i_0 = -2Fr_{overall,0} = -2Fk_1^{+,0} c_{H^+} N \frac{k_1^{0,+} c_{H^+} + k_2^{0,-} c_{H_2}}{k_1^{0,+} c_{H^+} + k_1^{0,-} + k_2^{0,+} c_{H^+} + k_2^{0,-} c_{H_2}} \tag{a.1.17}$$

A.2. Molecular hydrogen volmer-heyrovsky mechanism

The mechanism passing through the formation of hydrogen complexes in SAC consists of three elementary steps:

$$H^+ + e^- + * \underset{k_1^-}{\overset{k_1^+}{\rightleftharpoons}} H^* \tag{a.2.1}$$

$$H^* + H^+ + e^- \underset{k_2^-}{\overset{k_2^+}{\rightleftharpoons}} H_2^* \tag{a.2.2}$$

$$H_2^* \underset{k_3^-}{\overset{k_3^+}{\rightleftharpoons}} H_2 + * \tag{a.2.3}$$

where $k_3^+ = k_3^{+,0}$ and $k_3^- = k_3^{-,0}$ are the forward and backward kinetic constants of the chemical desorption step of molecular hydrogen.

The rate of each step is:

$$r_1 = r_1^+ - r_1^- = k_1^+ c_{H^+} N\left(1 - \theta_{H^*} - \theta_{H_2^*}\right) - k_1^- N\theta_{H^*} \tag{a.2.4}$$

$$r_2 = r_2^+ - r_2^- = k_2^+ c_{H^+} N\theta_{H^*} - k_2^- N\theta_{H_2^*} \tag{a.2.5}$$

$$r_3 = r_3^+ - r_3^- = k_3^+ N\theta_{H_2^*} - k_3^- c_{H_2} N\left(1 - \theta_{H^*} - \theta_{H_2^*}\right) \tag{a.2.6}$$

In the molecular hydrogen Volmer-Heyrovsky mechanism there are two intermediates: H* and H_2*. Then, steady-state assumption imposes:

$$\frac{d\theta_{H^*}}{dt} = \frac{r_1 - r_2}{N} = k_1^+ c_{H^+}\left(1 - \theta_{H^*} - \theta_{H_2^*}\right) - k_1^- \theta_{H^*} - k_2^+ c_{H^+}\theta_{H^*} + k_2^- \theta_{H_2^*} = 0 \tag{a.2.7}$$

$$\frac{d\theta_{H_2^*}}{dt} = \frac{r_2 - r_3}{N} = k_2^+ c_{H^+}\theta_{H^*} - k_2^- \theta_{H_2^*} - k_3^+ \theta_{H_2^*} + k_3^- c_{H_2}\left(1 - \theta_{H^*} - \theta_{H_2^*}\right) = 0 \tag{a.2.8}$$

An expression for intermediate coverage can be found by solving a system made by (a.2.7) and (a.2.8).

$$\theta_{H^*} = \frac{k_1^+ k_2^- c_{H^+} + k_1^+ k_3^+ c_{H^+} + k_2^- k_3^- c_{H_2}}{k_1^+ k_2^- c_{H^+} + k_1^+ k_3^+ c_{H^+} + k_2^- k_3^- c_{H_2} + k_1^+ k_2^+ c_{H^+}^2 + k_1^- k_2^- + k_1^- k_3^+ + k_2^- k_3^+ c_{H^+} + k_1^- k_3^- c_{H_2} + k_2^+ k_3^- c_{H^+} c_{H_2}} \tag{a.2.9}$$

$$\theta_{H_2^*} = \frac{k_1^+ k_2^+ c_{H^+}^2 + k_1^- k_3^- c_{H_2} + k_2^+ k_3^- c_{H^+} c_{H_2}}{k_1^+ k_2^- c_{H^+} + k_1^+ k_3^+ c_{H^+} + k_2^- k_3^- c_{H_2} + k_1^+ k_2^+ c_{H^+}^2 + k_1^- k_2^- + k_1^- k_3^+ + k_2^- k_3^+ c_{H^+} + k_1^- k_3^- c_{H_2} + k_2^+ k_3^- c_{H^+} c_{H_2}} \tag{a.2.10}$$

Substituting (a.2.9) and (a.2.10) in either (a.2.4), (a.2.5) or (a.2.6), it is possible to write an expression of overall rate.

$$r_{overall} = r_1 = k_1^+ c_{H^+} N \frac{k_1^- k_2^- + k_1^- k_3^+ + k_2^- k_3^+ c_{H^+}}{k_1^+ k_2^- c_{H^+} + k_1^+ k_3^+ c_{H^+} + k_2^- k_3^- c_{H_2} + k_1^+ k_2^+ c_{H^+}^2 + k_1^- k_2^- + k_1^- k_3^+ + k_2^- k_3^+ c_{H^+} + k_1^- k_3^- c_{H_2} + k_2^+ k_3^- c_{H^+} c_{H_2}} - k_1^- N \frac{k_1^+ k_2^- c_{H^+} + k_1^+ k_3^+ c_{H^+} + k_2^- k_3^- c_{H_2}}{k_1^+ k_2^- c_{H^+} + k_1^+ k_3^+ c_{H^+} + k_2^- k_3^- c_{H_2} + k_1^+ k_2^+ c_{H^+}^2 + k_1^- k_2^- + k_1^- k_3^+ + k_2^- k_3^+ c_{H^+} + k_1^- k_3^- c_{H_2} + k_2^+ k_3^- c_{H^+} c_{H_2}} \tag{a.2.11}$$

Current density is given by:

$$i_F = -2F \left[k_1^+ c_{H^+} N \frac{k_1^- k_2^- + k_1^- k_3^+ + k_2^- k_3^+ c_{H^+}}{k_1^+ k_2^- c_{H^+} + k_1^+ k_3^+ c_{H^+} + k_2^- k_3^- c_{H_2} + k_1^+ k_2^+ c_{H^+}^2 + k_1^- k_2^- + k_1^- k_3^+ + k_2^- k_3^+ c_{H^+} + k_1^- k_3^- c_{H_2} + k_2^+ k_3^- c_{H^+} c_{H_2}} - k_1^- N \frac{k_1^+ k_2^- c_{H^+} + k_1^+ k_3^+ c_{H^+} + k_2^- k_3^- c_{H_2}}{k_1^+ k_2^- c_{H^+} + k_1^+ k_3^+ c_{H^+} + k_2^- k_3^- c_{H_2} + k_1^+ k_2^+ c_{H^+}^2 + k_1^- k_2^- + k_1^- k_3^+ + k_2^- k_3^+ c_{H^+} + k_1^- k_3^- c_{H_2} + k_2^+ k_3^- c_{H^+} c_{H_2}} \right] \tag{a.2.12}$$

Similar to Volmer-Heyrovsky mechanism, it is possible to derive the expression of exchange current density.

$$H^+ + e^- + * \underset{k_1^{0,-}}{\overset{k_1^{0,+}}{\rightleftharpoons}} H^* \tag{a.2.13}$$

$$H^+ + H^* + e^- \underset{k_2^{0,-}}{\overset{k_2^{0,+}}{\rightleftharpoons}} H_2^* \tag{a.2.14}$$

$$H_2^* \underset{k_3^{0,-}}{\overset{k_3^{0,+}}{\rightleftharpoons}} H_2 + * \tag{a.2.15}$$

The rate of each step is:

$$r_{1,0} = r_{1,0}^+ - r_{1,0}^- = k_1^{+,0} c_{H^+} N\left(1 - \theta_{H^*,0} - \theta_{H_2^*,0}\right) - k_1^{-,0} N\theta_{H^*,0} \tag{a.2.16}$$

$$r_{2,0} = r_{2,0}^+ - r_{2,0}^- = k_2^+ c_{H^+} N\theta_{H^*,0} - k_2^{-,0} N\theta_{H_2^*,0} \tag{a.2.17}$$

$$r_{3,0} = r_{3,0}^+ - r_{3,0}^- = k_3^{+,0} N\theta_{H_2^*,0} - k_3^{-,0} c_{H_2} N\left(1 - \theta_{H^*,0} - \theta_{H_2^*,0}\right) \tag{a.2.18}$$

Steady-state assumption imposes:

$$\frac{d\theta_{H^*,0}}{dt} = \frac{r_{1,0} - r_{2,0}}{N} = k_1^{+,0} c_{H^+}\left(1 - \theta_{H^*,0} - \theta_{H_2^*,0}\right) - k_1^{-,0}\theta_{H^*,0} - k_2^+ c_{H^+}\theta_{H^*,0} + k_2^{-,0}\theta_{H_2^*,0} = 0 \tag{a.2.19}$$

$$\frac{d\theta_{H_2^*,0}}{dt} = \frac{r_{2,0} - r_{3,0}}{N} = k_2^+ c_{H^+}\theta_{H^*,0} - k_2^{-,0}\theta_{H_2^*,0} - k_3^{+,0}\theta_{H_2^*,0} + k_3^{-,0} c_{H_2}\left(1 - \theta_{H^*,0} - \theta_{H_2^*,0}\right) = 0 \tag{a.2.20}$$

Solving the system made by (a.2.19) and (a.2.20), it is possible to obtain:

$$\theta_{H^*,0} = \frac{k_1^{+,0} k_2^{-,0} c_{H^+} + k_1^{+,0} k_3^{+,0} c_{H^+} + k_2^{-,0} k_3^{-,0} c_{H_2}}{k_1^{+,0} k_2^{-,0} c_{H^+} + k_1^{+,0} k_3^{+,0} c_{H^+} + k_2^{-,0} k_3^{-,0} c_{H_2} + k_1^{+,0} k_2^{+,0} c_{H^+}^2 + k_1^{-,0} k_2^{-,0} + k_1^{-,0} k_3^{+,0} + k_2^{-,0} k_3^{+,0} c_{H^+} + k_1^{-,0} k_3^{-,0} c_{H_2} + k_2^{+,0} k_3^{-,0} c_{H^+} c_{H_2}} \tag{a.2.21}$$

$$\theta_{H_2^*,0} = \frac{k_1^{+,0}k_2^{+,0}c_{H^+}^2 + k_1^{-,0}k_3^{-,0}c_{H_2} + k_2^{+,0}k_3^{-,0}c_{H^+}c_{H_2}}{k_1^{+,0}k_2^{-,0}c_{H^+} + k_1^{+,0}k_3^{+,0}c_{H^+} + k_2^{-,0}k_3^{-,0}c_{H_2} + k_1^{+,0}k_2^{+,0}c_{H^+}^2 + k_1^{-,0}k_2^{-,0} + k_1^{-,0}k_3^{+,0} + k_2^{-,0}k_3^{+,0}c_{H^+} + k_1^{-,0}k_3^{-,0}c_{H_2} + k_2^{+,0}k_3^{-,0}c_{H^+}c_{H_2}} \tag{a.2.22}$$

Finally, it is possible to obtain the expression of the overall rate at zero polarization potential and then, substituting into (a.2.12), the exchange density current.

$$r_{overall} = r_1^{+,0} = k_1^{+,0}c_{H^+}N\frac{k_1^{+,0}k_2^{-,0}c_{H^+} + k_1^{+,0}k_3^{+,0}c_{H^+} + k_2^{-,0}k_3^{-,0}c_{H_2}}{k_1^{+,0}k_2^{-,0}c_{H^+} + k_1^{+,0}k_3^{+,0}c_{H^+} + k_2^{-,0}k_3^{-,0}c_{H_2} + k_1^{+,0}k_2^{+,0}c_{H^+}^2 + k_1^{-,0}k_2^{-,0} + k_1^{-,0}k_3^{+,0} + k_2^{-,0}k_3^{+,0}c_{H^+} + k_1^{-,0}k_3^{-,0}c_{H_2} + k_2^{+,0}k_3^{-,0}c_{H^+}c_{H_2}} \tag{a.2.23}$$

$$i = -2Fk_1^{+,0}c_{H^+}N\frac{k_1^{+,0}k_2^{-,0}c_{H^+} + k_1^{+,0}k_3^{+,0}c_{H^+} + k_2^{-,0}k_3^{-,0}c_{H_2}}{k_1^{+,0}k_2^{-,0}c_{H^+} + k_1^{+,0}k_3^{+,0}c_{H^+} + k_2^{-,0}k_3^{-,0}c_{H_2} + k_1^{+,0}k_2^{+,0}c_{H^+}^2 + k_1^{-,0}k_2^{-,0} + k_1^{-,0}k_3^{+,0} + k_2^{-,0}k_3^{+,0}c_{H^+} + k_1^{-,0}k_3^{-,0}c_{H_2} + k_2^{+,0}k_3^{-,0}c_{H^+}c_{H_2}} \tag{a.2.24}$$

A.3. 1D diffusion correction

Levich equation allows to linearly correlate the Faradaic current density with c_{H^+} at electrode surface:

$$i_F(c_{H^+}) = 0.0620nFD_H^{\frac{2}{3}}\Omega^{\frac{1}{2}}\nu^{-\frac{1}{6}}\left(c_{H^+} - c_{H^+}^{bulk}\right) \tag{a.3.1}$$

Where Ω is the rotation rate, ν is the kinematic viscosity, $c_{H^+}^{bulk}$ is the reactant concentration in bulk and c_{H^+} is the reactant concentration at electrode surface. From (a.3.1) it is possible to define a function that is c_{H^+}-dependent that can be used for a convergence algorithm based on Newton-Raphson method.

$$f(c_{H^+}) = \frac{J_{H^+}(c_{H^+})}{\left(0.0620D_H^{\frac{2}{3}}\Omega^{\frac{1}{2}}\nu^{-\frac{1}{6}}\right)} + c_{H^+}^{bulk} - c_{H^+} \tag{a.3.2}$$

Where $J_{H^+}(c_{H^+}) = i_F(c_{H^+})/nF$ and represents the flux of H^+ from bulk to electrode surface. The updated value of c_{H^+} is defined as:

$$c_{H^+}^{i+1} = c_{H^+}^{i} - \frac{f(c_{H^+}^{i})}{f'(c_{H^+}^{i})} \tag{a.3.3}$$

After achieving the convergence for c_{H^+}, it is possible to determine the value of c_{H_2} at the same potential applying thermodynamic consistency. For HER, reaction quotient is defined as:

$$Q = \frac{c_{H_2}}{c_{H^+}^2} \tag{a.3.4}$$

Reaction Gibbs free energy can be written as:

$$\Delta G_r = \Delta G_r^{\circ} + RTlnQ \tag{a.3.5}$$

Where ΔG_r° is zero for HER. From (a.3.5) reaction quotient can be also written as:

$$Q = e^{-\frac{\Delta G_r}{RT}} \tag{a.3.6}$$

Since $\Delta G_r = -nF\phi$, substituting (a.3.6) in (a.3.4), it is possible to find an expression for c_{H_2}.

$$c_{H_2} = c_{H^+}^2\exp\left(-\frac{nF\phi}{RT}\right) \tag{a.3.7}$$

B. Electrochemical impedance spectroscopy modeling

B.1. Diffusion-free volmer-heyrovsky model

Electrochemical Faradaic admittance ($Y_F = 1/Z_F$, Z_F is Faradaic impedance) can be defined as:

$$\frac{1}{Z_F} = \frac{\widetilde{i}_F}{\widetilde{\phi}} \tag{b.1.1}$$

Where $\widetilde{i}_F$ is the phasor of i_F and $\widetilde{\phi}$ is the phasor of ϕ. In the case of Volmer-Heyrovsky mechanism, without considering diffusion phenomena, Faradaic

current density can be expressed in function of polarization potential and adsorbed hydrogen coverage:

$$i_F = i_F(\phi, \theta_{H^*}) \tag{b.1.2}$$

Then, we can write Faradaic current density with a first order Taylor series expansion with respect to steady-state values of applied potential (ϕ^*) and H* coverage ($\theta^*_{H^*}$).

$$i_F = i^*_F + \left(\frac{\partial i_F}{\partial \phi}\right)_{\theta^*_{H^*}} (\phi - \phi^*) + \left(\frac{\partial i_F}{\partial \theta_{H^*}}\right)_{\phi^*} \left(\theta_{H^*} - \theta^*_{H^*}\right) \tag{b.1.3}$$

We define the potential perturbation $\Delta\phi = (\phi - \phi^*)$ and coverage perturbation $\Delta\theta_{H^*} = \left(\theta_{H^*} - \theta^*_{H^*}\right)$. A time-dependent term like $i_F(t)$ can be expressed in terms of steady-state value (i^*_F) and a sinusoidal time-dependent contribution:

$$i_F = i^*_F + |i_F|\cos(\omega t + \varphi) \tag{b.1.4}$$

Where $|i_F|$ is the magnitude of the perturbation, ω is angular frequency and φ is phase shift. Applying Euler's formula, $e^{j\alpha} = \cos(\alpha) + j\sin(\alpha)$ (where j is imaginary unit), (b.1.4) can also be expressed as:

$$\Delta i_F = i_F - i^*_F = Re\left\{\widetilde{i}_F e^{j\omega t}\right\} \tag{b.1.5}$$

Where $\widetilde{i}_F = |i_F|e^{j\varphi}$. A similar expression for $\Delta\phi$ and $\Delta\theta_{H^*}$ can be easily found.

Substituting (b.1.5) in (b.1.3) and dividing by $\widetilde{\phi}$, we obtain a new expression of Faradaic admittance:

$$Y_F = \frac{\widetilde{i}_F}{\widetilde{\phi}} = \left(\frac{\partial i_F}{\partial \phi}\right)_{\theta^*_{H^*}} + \left(\frac{\partial i_F}{\partial \theta_{H^*}}\right)_{\phi^*} \frac{\widetilde{\theta}_{H^*}}{\widetilde{\phi}} \tag{b.1.6}$$

$\frac{\widetilde{\theta}_{H^*}}{\widetilde{\phi}}$ is the only unknown term of (b.1.6). Then, to find its expression we can write first order Taylor series expansion of the function $g(\phi,\ \theta_{H^*})$, defined as $g = \frac{d\theta_{H^*}}{dt}$, with respect to steady-state values of polarization potential and H* coverage.

$$g(\phi, \theta_H) = g\left(\phi^*, \theta^*_H\right) + \left(\frac{\partial g}{\partial \phi}\right)_{\theta^*_{H^*}} \Delta\phi + \left(\frac{\partial g}{\partial \theta_{H^*}}\right)_{\phi^*} \Delta\theta_{H^*} \tag{b.1.7}$$

Where $g\left(\phi^*, \theta^*_H\right) = 0$. It is possible to express $g(\phi, \theta_H)$ also as:

$$g(\phi, \theta_H) = \frac{d\theta_{H^*}}{dt} = \frac{d}{dt}\left(\theta^*_{H^*} + \Delta\theta_{H^*}\right) = \frac{d\Delta\theta_{H^*}}{dt} = j\omega\widetilde{\theta}_{H^*} e^{j\omega t} \tag{b.1.8}$$

Substituting (b.1.8) into (b.1.7), expressing potential and coverage perturbations in exponential form, and dividing by $\widetilde{\phi}$, it is possible to obtain:

$$j\omega\frac{\widetilde{\theta}_{H^*}}{\widetilde{\phi}} = \left(\frac{\partial g}{\partial \phi}\right)_{\theta^*_{H^*}} + \left(\frac{\partial g}{\partial \theta_{H^*}}\right)_{\phi^*} \frac{\widetilde{\theta}_{H^*}}{\widetilde{\phi}} \tag{b.1.9}$$

Isolating $\frac{\widetilde{\theta}_{H^*}}{\widetilde{\phi}}$ from (b.1.9) we obtain:

$$\frac{\widetilde{\theta}_{H^*}}{\widetilde{\phi}} = \frac{\left(\frac{\partial g}{\partial \phi}\right)_{\theta^*_{H^*}}}{j\omega - \left(\frac{\partial g}{\partial \theta_{H^*}}\right)_{\phi^*}} \tag{b.1.10}$$

Substituting (b.1.10) into (b.1.6), it is possible to write the expression of Faradaic admittance for Volmer-Heyrovsky mechanism in the absence of diffusion correction.

$$\frac{1}{Z_F} = \left(\frac{\partial i_F}{\partial \phi}\right)_{\theta^*_{H^*}} + \left(\frac{\partial i_F}{\partial \theta_{H^*}}\right)_{\phi^*} \frac{\left(\frac{\partial g}{\partial \phi}\right)_{\theta^*_{H^*}}}{j\omega - \left(\frac{\partial g}{\partial \theta_{H^*}}\right)_{\phi^*}} \tag{b.1.11}$$

B.2. Diffusion-free molecular hydrogen volmer-heyrovsky model

Faradaic current density can be expressed in function of polarization potential and adsorbed hydrogen and hydrogen complexes coverage:

$$i_F = i_F\left(\phi, \theta_{H^*}, \theta_{H_2^*}\right) \tag{b.2.1}$$

Similar to the previous case of Volmer-Heyrovsky mechanism, adopting a first order Taylor series expansion of i_F, it is possible to find an expression of Faradaic admittance.

$$\frac{1}{Z_F} = \left(\frac{\partial i_F}{\partial \phi}\right)_{\theta^*_{H^*},\theta^*_{H_2^*}} + \left(\frac{\partial i_F}{\partial \theta_{H^*}}\right)_{\phi^*,\theta^*_{H_2^*}} \frac{\widetilde{\theta}_{H^*}}{\widetilde{\phi}} + \left(\frac{\partial i_F}{\partial \theta_{H_2^*}}\right)_{\phi^*,\theta^*_{H^*}} \frac{\widetilde{\theta}_{H_2^*}}{\widetilde{\phi}} \tag{b.2.2}$$

$\frac{\widetilde{\theta}_{H^*}}{\widetilde{\phi}}$ and $\frac{\widetilde{\theta}_{H_2^*}}{\widetilde{\phi}}$ are unknown terms of (b.2.2). Then, to find their expressions we can write the first order Taylor series expansion of the functions $g\left(\phi,\ \theta_{H^*},\ \theta_{H_2^*}\right)$, defined as $g = \frac{d\theta_{H^*}}{dt}$, and $q\left(\phi,\ \theta_{H^*},\theta_{H_2^*}\right)$, defined as $q = \frac{d\theta_{H_2^*}}{dt}$, with respect to steady-state values of polarization potential, H* and H_2* coverages.

$$g\left(\phi,\ \theta_{H^*},\theta_{H_2^*}\right) = \left(\frac{\partial g}{\partial \phi}\right)_{\theta^*_{H^*},\theta^*_{H_2^*}} + \left(\frac{\partial g}{\partial \theta_{H^*}}\right)_{\phi^*,\theta^*_{H_2^*}} \Delta\theta_{H^*} + \left(\frac{\partial g}{\partial \theta_{H_2^*}}\right)_{\phi^*,\theta^*_{H^*}} \Delta\theta_{H_2^*} \tag{b.2.3}$$

$$q\left(\phi,\ \theta_{H^*},\theta_{H_2^*}\right) = \left(\frac{\partial q}{\partial \phi}\right)_{\theta^*_{H^*},\theta^*_{H_2^*}} + \left(\frac{\partial q}{\partial \theta_{H^*}}\right)_{\phi^*,\theta^*_{H_2^*}} \Delta\theta_{H^*} + \left(\frac{\partial q}{\partial \theta_{H_2^*}}\right)_{\phi^*,\theta^*_{H^*}} \Delta\theta_{H_2^*} \tag{b.2.4}$$

But it is possible to express $g\left(\phi,\ \theta_{H^*},\theta_{H_2^*}\right)$ and $q\left(\phi,\ \theta_{H^*},\theta_{H_2^*}\right)$ also in another way:

$$g\left(\phi,\ \theta_{H^*},\theta_{H_2^*}\right) = \frac{d\theta_{H^*}}{dt} = \frac{d}{dt}\left(\theta^*_{H^*} + \Delta\theta_{H^*}\right) = j\omega\widetilde{\theta}_{H^*}e^{j\omega t} \tag{b.2.5}$$

$$q\left(\phi,\ \theta_{H^*},\theta_{H_2^*}\right) = \frac{d\theta_{H_2^*}}{dt} = \frac{d}{dt}\left(\theta^*_{H_2^*} + \Delta\theta_{H_2^*}\right) = j\omega\widetilde{\theta}_{H_2^*}e^{j\omega t} \tag{b.2.6}$$

Substituting (b.2.5) in (b.2.3) and (b.2.6) in (b.2.4), and dividing by $\widetilde{\phi}$, it is possible to write:

$$j\omega\frac{\widetilde{\theta}_{H^*}}{\widetilde{\phi}} = \left(\frac{\partial g}{\partial \phi}\right)_{\theta^*_{H^*},\theta^*_{H_2^*}} + \left(\frac{\partial g}{\partial \theta_{H^*}}\right)_{\phi^*,\theta^*_{H_2^*}} \frac{\widetilde{\theta}_{H^*}}{\widetilde{\phi}} + \left(\frac{\partial g}{\partial \theta_{H_2^*}}\right)_{\phi^*,\theta^*_{H^*}} \frac{\widetilde{\theta}_{H_2^*}}{\widetilde{\phi}} \tag{b.2.7}$$

$$j\omega\frac{\widetilde{\theta}_{H_2^*}}{\widetilde{\phi}} = \left(\frac{\partial q}{\partial \phi}\right)_{\theta^*_{H^*},\theta^*_{H_2^*}} + \left(\frac{\partial q}{\partial \theta_{H^*}}\right)_{\phi^*,\theta^*_{H_2^*}} \frac{\widetilde{\theta}_{H^*}}{\widetilde{\phi}} + \left(\frac{\partial q}{\partial \theta_{H_2^*}}\right)_{\phi^*,\theta^*_{H^*}} \frac{\widetilde{\theta}_{H_2^*}}{\widetilde{\phi}} \tag{b.2.8}$$

Solving the system of equation made by (b.2.7) and (b.2.8), we find the expression of $\frac{\widetilde{\theta}_{H^*}}{\widetilde{\phi}}$ and $\frac{\widetilde{\theta}_{H_2^*}}{\widetilde{\phi}}$.

$$\frac{\widetilde{\theta}_{H^*}}{\widetilde{\phi}} = \frac{-\left(\frac{\partial g}{\partial \theta_{H_2^*}}\right)_{\phi^*,\theta^*_{H^*}}\left(\frac{\partial q}{\partial \phi}\right)_{\theta^*_{H^*},\theta^*_{H_2^*}} - j\omega\left(\frac{\partial g}{\partial \phi}\right)_{\theta^*_{H^*},\theta^*_{H_2^*}} + \left(\frac{\partial g}{\partial \phi}\right)_{\theta^*_{H^*},\theta^*_{H_2^*}}\left(\frac{\partial q}{\partial \theta_{H_2^*}}\right)_{\phi^*,\theta^*_{H^*}}}{\left(\frac{\partial g}{\partial \theta_{H_2^*}}\right)_{\theta^*_{H^*},\theta^*_{H_2^*}}\left(\frac{\partial q}{\partial \theta_{H^*}}\right)_{\phi^*,\theta^*_{H_2^*}} + j\omega\left(\frac{\partial g}{\partial \theta_{H^*}}\right)_{\phi^*,\theta^*_{H_2^*}} + \omega^2 - \left(\frac{\partial g}{\partial \theta_{H^*}}\right)_{\phi^*,\theta^*_{H_2^*}}\left(\frac{\partial q}{\partial \theta_{H_2^*}}\right)_{\phi^*,\theta^*_{H^*}} + j\omega\left(\frac{\partial q}{\partial \theta_{H_2^*}}\right)_{\phi^*,\theta^*_{H^*}}} \tag{b.2.9}$$

$$\frac{\widetilde{\theta}_{H_2^*}}{\widetilde{\phi}} = \frac{\left(\frac{\partial g}{\partial \theta_{H^*}}\right)_{\phi^*,\theta^*_{H_2^*}}\left(\frac{\partial q}{\partial \phi}\right)_{\theta^*_{H^*},\theta^*_{H_2^*}} - \left(\frac{\partial g}{\partial \phi}\right)_{\theta^*_{H^*},\theta^*_{H_2^*}}\left(\frac{\partial q}{\partial \theta_{H^*}}\right)_{\phi^*,\theta^*_{H_2^*}} - j\omega\left(\frac{\partial q}{\partial \phi}\right)_{\theta^*_{H^*},\theta^*_{H_2^*}}}{\left(\frac{\partial g}{\partial \theta_{H_2^*}}\right)_{\theta^*_{H^*},\theta^*_{H_2^*}}\left(\frac{\partial q}{\partial \theta_{H^*}}\right)_{\phi^*,\theta^*_{H_2^*}} + j\omega\left(\frac{\partial g}{\partial \theta_{H^*}}\right)_{\phi^*,\theta^*_{H_2^*}} + \omega^2 - \left(\frac{\partial g}{\partial \theta_{H^*}}\right)_{\phi^*,\theta^*_{H_2^*}}\left(\frac{\partial q}{\partial \theta_{H_2^*}}\right)_{\phi^*,\theta^*_{H^*}} + j\omega\left(\frac{\partial q}{\partial \theta_{H_2^*}}\right)_{\phi^*,\theta^*_{H^*}}} \tag{b.2.10}$$

Substituting (b.2.9) and (b.2.10) in (b.2.2), it is possible to write the final expression of Faradaic admittance for Volmer-Heyrovsky mechanism mediated by the formation of hydrogen complexes.

$$\frac{1}{Z_F} = \left(\frac{\partial i_F}{\partial \phi}\right)_{\theta^*_{H^*},\theta^*_{H_2^*}} + \left(\frac{\partial i_F}{\partial \theta_{H^*}}\right)_{\phi^*,\theta^*_{H_2^*}} \frac{-\left(\frac{\partial g}{\partial \theta_{H_2^*}}\right)_{\phi^*,\theta^*_{H^*}} \left(\frac{\partial q}{\partial \phi}\right)_{\theta^*_{H^*},\theta^*_{H_2^*}} - j\omega\left(\frac{\partial g}{\partial \phi}\right)_{\theta^*_{H^*},\theta^*_{H_2^*}} + \left(\frac{\partial g}{\partial \phi}\right)_{\theta^*_{H^*},\theta^*_{H_2^*}} \left(\frac{\partial q}{\partial \theta_{H_2^*}}\right)_{\phi^*,\theta^*_{H^*}}}{\left(\frac{\partial g}{\partial \theta_{H_2^*}}\right)_{\theta^*_{H^*},\theta^*_{H_2^*}} \left(\frac{\partial q}{\partial \theta_{H^*}}\right)_{\phi^*,\theta^*_{H_2^*}} + j\omega\left(\frac{\partial g}{\partial \theta_{H^*}}\right)_{\phi^*,\theta^*_{H_2^*}} + \omega^2 - \left(\frac{\partial g}{\partial \theta_{H^*}}\right)_{\phi^*,\theta^*_{H_2^*}} \left(\frac{\partial q}{\partial \theta_{H_2^*}}\right)_{\phi^*,\theta^*_{H^*}} + j\omega\left(\frac{\partial q}{\partial \theta_{H_2^*}}\right)_{\phi^*,\theta^*_{H^*}}} + \left(\frac{\partial i_F}{\partial \theta_{H_2^*}}\right)_{\phi^*,\theta^*_{H^*}} \frac{\left(\frac{\partial g}{\partial \theta_{H^*}}\right)_{\phi^*,\theta^*_{H_2^*}} \left(\frac{\partial q}{\partial \phi}\right)_{\theta^*_{H^*},\theta^*_{H_2^*}} - \left(\frac{\partial g}{\partial \phi}\right)_{\theta^*_{H^*},\theta^*_{H_2^*}} \left(\frac{\partial q}{\partial \theta_{H^*}}\right)_{\phi^*,\theta^*_{H_2^*}} - j\omega\left(\frac{\partial q}{\partial \phi}\right)_{\theta^*_{H^*},\theta^*_{H_2^*}}}{\left(\frac{\partial g}{\partial \theta_{H_2^*}}\right)_{\theta^*_{H^*},\theta^*_{H_2^*}} \left(\frac{\partial q}{\partial \theta_{H^*}}\right)_{\phi^*,\theta^*_{H_2^*}} + j\omega\left(\frac{\partial g}{\partial \theta_{H^*}}\right)_{\phi^*,\theta^*_{H_2^*}} + \omega^2 - \left(\frac{\partial g}{\partial \theta_{H^*}}\right)_{\phi^*,\theta^*_{H_2^*}} \left(\frac{\partial q}{\partial \theta_{H_2^*}}\right)_{\phi^*,\theta^*_{H^*}} + j\omega\left(\frac{\partial q}{\partial \theta_{H_2^*}}\right)_{\phi^*,\theta^*_{H^*}}} \tag{b.2.11}$$

B.3. Diffusion model choice and its validity

To describe better the chemistry of the process it is important to add diffusion correction to our models. Different from the previous cases of diffusion corrected steady-state microkinetic models, it is not enough just to estimate the value of c_{H^+} and c_{H_2} at the electrode surface under steady-state conditions, but it must also be considered that c_{H^+} and c_{H_2} are time-dependent. This means that also active species' concentrations are perturbated by the application of a potential perturbation to the system. The use of Levich equation (see A.3) implies the presence of a finite length diffusion. That said, we decided to include a semi-infinite diffusion in our impedance model, in order to simplify the equations involved. From a practical point of view, this is a good approximation of the system if the penetration depth generated by the alternating signal used for the impedance study is small enough. Such depth is defined as:

$$\delta_l = \sqrt{\frac{D}{\omega}} \tag{b.3.1}$$

where D represents the diffusion coefficient of the species in exam (in this case H^+) and ω is the angular frequency used in the impedance analysis. The value of δ_l is to be compared to the thickness of the diffusion layer L_d which can be calculated from Levich's equation:

$$L_d = 1.61 D^{\frac{1}{3}} \upsilon^{\frac{1}{6}} \Omega^{-\frac{1}{2}} \tag{b.3.2}$$

where υ is the kinematic viscosity and Ω the rotation speed of the RDE. When $\delta_l \ll L_d$ the effect of the bound is not felt, and the diffusion behave like in the semi-infinite case. In the case of mono-dimensional diffusion, the diffusion impedance can be written in the following form: [87]

$$Z_d = \frac{RT}{n^2F^2} \frac{\lambda_L}{c\sqrt{D}} (j\omega)^{-\frac{1}{2}} \tag{b.3.3}$$

where R is the gas constant, T is the temperature, n the valency, F the Faraday's constant, c the concentration of the moving species, and j the imaginary unit. In the two case limits of reflective and transmissive boundary the factor λ_L is either $coth\left(\frac{L_d}{\delta_l}\right)$ or $tanh\left(\frac{L_d}{\delta_l}\right)$ respectively, both approaching a value of 1 when $\frac{L_d}{\delta_l} \geq 3$, which ultimately translates in equation b.3.3 simplifying as that of semi-infinite diffusion. Finally, the limit frequency below which the semi-infinite diffusion approximation holds can be calculated as follows:

$$\omega_{limit} = 3.47 D^{\frac{1}{3}} \upsilon^{-\frac{1}{3}} \Omega \tag{b.3.4}$$

Fig. B1 reports the magnitude of the impedance spectra calculated at different RDE rotation speed and at −0.4 V for the two models, together with the limit frequency for semi-infinite diffusion approximation. The following considerations can be drawn up:

- As previously mentioned (see Fig. 4 and the relative discussion), diffusion only plays a role in the pure Volmer-Heyrovsky model (upper panel of Fig. B1), and only at very low potential.
- The limit frequency for semi-infinite approximation validity scales linearly with the rotation speed of the RDE, reaching circa 100 Hz at 1000 rpm (which is the value used for all the simulations in this work).

Although this frequency is relatively high, it is possible to observe that most of the information of the model (i.e., the whole region associated with the semicircle in the Nyquist plot) appears to be contained in the higher frequencies.

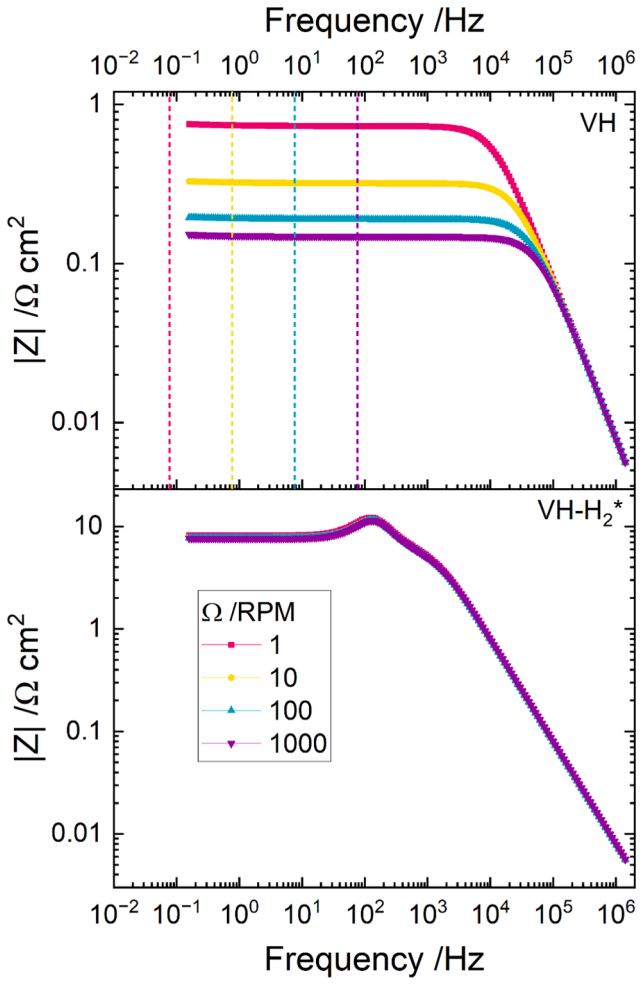

Fig. B1. Comparison between the Bode plots (only |Z|) of the impedance simulated at different rotation speed of the RDE for the two models. The upper panel (Volmer-Heyrovsky model) also features the respective limit frequencies for semi-infinite diffusion, as calculated from equation b.3.4.

This is clearly seen in Fig. B2, where the Nyquist plot from a spectrum simulated with rotation speed equals to 1000 rpm and potential equals to −0.4 V is shown.

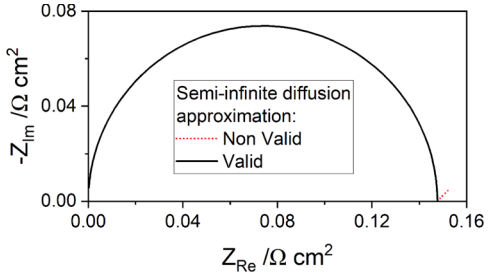

Fig. B2. Nyquist plot of an impedance spectrum simulated with the VH model, rotation speed equals to 1000 rpm and potential equals to −0.4 V. The portion of the spectrum where diffusion can be approximated as semi-infinite is shown as a straight black line, while red dotted line is used where it is not.

B.4. 1D diffusion corrected volmer-heyrovsky model

Taking into account all considerations made in the previous section, it is possible to express the Faradaic current density as:

$$i_F = i_F(\phi, \theta_{H^*}, c_{H^+}, c_{H_2}) \tag{b.4.1}$$

The first order Taylor series expansion applied to (b.4.1) brings to the expression of Faradaic admittance.

$$\frac{1}{Z_F} = \left(\frac{\partial i_F}{\partial \phi}\right)_{\theta_{H^*}, c_{H^+}, c_H 2} + \left(\frac{\partial i_F}{\partial \theta_{H^*}}\right)_{\phi^*, c_{H^+}, c_H 2} \frac{\widetilde{\theta}_{H^*}}{\widetilde{\phi}} + \left(\frac{\partial i_F}{\partial c_{H^+}}\right)_{\phi^*, \theta_{H^*}, c_H 2} \frac{\widetilde{c}_{H^+}}{\widetilde{\phi}} + \left(\frac{\partial i_F}{\partial c_{H_2}}\right)_{\phi^*, \theta_{H^*} c_{H^+}} \frac{\widetilde{c}_{H_2}}{\widetilde{\phi}} \tag{b.4.2}$$

To find $\widetilde{c}_{H^+}$ it is possible to solve a set of Fick's laws, applied to flux and concentration perturbations of H^+ and H_2. D_{H^+} and D_{H_2} are diffusion coefficients associated with H^+ and H_2.

$$\Delta J_{H^+}(x,t) = -D_{H^+}\frac{\partial \Delta c_{H^+}(x,t)}{\partial x} \tag{b.4.3}$$

$$\frac{\partial \Delta c_{H^+}(x,t)}{\partial t} = D_{H^+}\frac{\partial^2 \Delta c_{H^+}(x,t)}{\partial x^2} \tag{b.4.4}$$

$$\Delta J_{H_2}(x,t) = -D_{H_2}\frac{\partial \Delta c_{H_2}(x,t)}{\partial x} \tag{b.4.5}$$

$$\frac{\partial \Delta c_{H_2}(x,t)}{\partial t} = D_{H_2}\frac{\partial^2 \Delta c_{H_2}(x,t)}{\partial x^2} \tag{b.4.6}$$

Making the Fourier transformation to (b.4.3)-(b.4.6) involves applying the following operations:

$$\mathscr{F}_t\{f(x,t)\} = f(x,\omega) \tag{b.4.7}$$

$$\mathscr{F}_t\left\{\frac{\partial f(x,t)}{\partial x}\right\} = \frac{\partial f(x,\omega)}{\partial x} \tag{b.4.8}$$

$$\mathscr{F}_t\left\{\frac{\partial f(x,t)}{\partial t}\right\} = j\omega\frac{\partial f(x,\omega)}{\partial t} \tag{b.4.9}$$

Applying (b.4.7)- (b.4.9) to (b.4.3)-(b.4.6), it is possible to obtain a new set of Fick's laws in terms of frequency-dependent fluxes and concentrations.

$$\Delta J_{H^+}(x,\omega) = -D_{H^+}\frac{\partial \Delta c_{H^+}(x,\omega)}{\partial x} \tag{b.4.10}$$

$$j\omega\Delta c_{H^+}(x,\omega) = D_{H^+}\frac{\partial^2 \Delta c_{H^+}(x,\omega)}{\partial x^2} \tag{b.4.11}$$

$$\Delta J_{H_2}(x,\omega) = -D_{H_2}\frac{\partial \Delta c_{H_2}(x,\omega)}{\partial x} \tag{b.4.12}$$

$$j\omega\Delta c_{H_2}(x,\omega) = D_{H_2}\frac{\partial^2 \Delta c_{H_2}(x,\omega)}{\partial x^2} \tag{b.4.13}$$

Solutions for (b.4.11) and (b.4.13) have the following expressions:

$$\Delta c_{H^+}(x,\omega) = M(\omega)e^{x\sqrt{\frac{j\omega}{D_{H^+}}}} + N(\omega)e^{-x\sqrt{\frac{j\omega}{D_{H^+}}}} \tag{b.4.14}$$

$$\Delta c_{H_2}(x,\omega) = M'(\omega)e^{x\sqrt{\frac{j\omega}{D_{H_2}}}} + N'(\omega)e^{-x\sqrt{\frac{j\omega}{D_{H_2}}}} \tag{b.4.15}$$

We can impose the following boundary conditions for H^+:

$$If\ x = \infty:\ \Delta c_{H^+}(x,\omega) = 0 \tag{b.4.16}$$

$$If\ x = 0:\ \Delta J_{H^+}(x,\omega) = \Delta(-r_1 - r_2) \tag{b.4.17}$$

And for H_2:

$$If\ x = \infty:\ \Delta c_{H_2}(x,\omega) = 0 \tag{b.4.18}$$

$$If\ x = 0:\ \Delta J_{H_2}(x,\omega) = \Delta r_2 \tag{b.4.19}$$

From (b.4.16) and (b.4.17) we obtain:

$$\Delta c_{H^+}(x,\omega) = N(\omega)e^{-x\sqrt{\frac{j\omega}{D_{H^+}}}} \tag{b.4.20}$$

$$\Delta(-r_1 - r_2) = D_{H^+}\sqrt{\frac{j\omega}{D_{H^+}}}\Delta c_{H^+}(x,\omega) \tag{b.4.21}$$

And from (b.4.18) and (b.4.19) we obtain:

$$\Delta c_{H_2}(x,\omega) = N'(\omega)e^{-x\sqrt{\frac{j\omega}{D_{H_2}}}} \tag{b.4.22}$$

$$\Delta r_2 = D_{H_2}\sqrt{\frac{j\omega}{D_{H_2}}}\Delta c_{H_2}(x,\omega) \tag{b.4.23}$$

The notation $\Delta c_{H^+}(x,\omega)$ (or $\Delta c_{H_2}(x,\omega)$) simply denotes the phasor $\widetilde{c}_{H^+}$ (or $\widetilde{c}_{H_2}$), which is the frequency-dependent term of the concentration perturbation after Fourier transform. In fact, Fourier transform is defined as:

$$\mathscr{F}_t\{f(t)\} \equiv \int_{-\infty}^{+\infty} f(t)e^{-j\omega t}dt \tag{b.4.24}$$

And applying (b.4.24) to $\Delta c_{H^+}(x,t)$ brings to:

$$\mathscr{F}_t\{\Delta c_{H^+}(x,t)\} = \mathscr{F}_t\left\{\widetilde{c}_{H^+}e^{j\omega t}\right\} = \widetilde{c}_{H^+} \tag{b.4.25}$$

It is important to underline that, under the conditions chosen for the simulation, the Fourier transform produces the same effect as the Laplace transform, another transform typically used in signal processing. In fact, we assume steady-state is reached before the application of ac sine-wave signals (i.e., complex variable $s = j\omega$ with no transient component). Moreover, we assume periodic perturbations with a domain big enough (i.e., ac current and potential measured for enough periods) so that they can be approximated as infinite. Under such conditions, the two transform deliver the same result.

Defining $w = -r_1 - r_2$, it is possible to rewrite Δw and Δr_2 with a first order Taylor series expansion. The expression of $r_1(\phi, \theta_{H^*}, c_{H^+})$ and $r_2(\phi, \theta_{H^*}, c_{H^+}, c_{H_2})$ is defined by (a.1.3) and (a.1.4) from the microkinetic discussion.

$$\Delta w = \left(\frac{\partial w}{\partial \phi}\right)_{\theta^*_{H^*}, c^*_{H^+}, c^*_H 2} + \left(\frac{\partial w}{\partial \theta_{H^*}}\right)_{\phi^*, c^*_{H^+}, c^*_H 2}\Delta\theta_{H^*} + \left(\frac{\partial w}{\partial c_{H^+}}\right)_{\phi^*, \theta^*_{H^*}, c^*_H 2}\Delta c_{H^+} + \left(\frac{\partial w}{\partial c_{H_2}}\right)_{\phi^*, \theta^*_{H^*} c^*_{H^+}}\Delta c_{H_2} \tag{b.4.26}$$

$$\Delta r_2 = \left(\frac{\partial r_2}{\partial \phi}\right)_{\theta^*_{H^*}, c^*_{H^+}, c^*_H 2} + \left(\frac{\partial r_2}{\partial \theta_{H^*}}\right)_{\phi^*, c^*_{H^+}, c^*_H 2}\Delta\theta_{H^*} + \left(\frac{\partial r_2}{\partial c_{H^+}}\right)_{\phi^*, \theta^*_{H^*}, c^*_H 2}\Delta c_{H^+} + \left(\frac{\partial r_2}{\partial c_{H_2}}\right)_{\phi^*, \theta^*_{H^*} c^*_{H^+}}\Delta c_{H_2} \tag{b.4.27}$$

Substituting (b.4.26) in (b.4.21) and (b.4.27) in (b.4.23), expressing perturbation terms with exponential form, and dividing by $\widetilde{\phi}$, it is possible to write:

$$D_{H^+}\sqrt{\frac{j\omega}{D_{H^+}}}\,\frac{\widetilde{c}_{H^+}}{\widetilde{\phi}} = \left(\frac{\partial w}{\partial \phi}\right)_{\theta^*_{H^*}, c^*_{H^+}, c^*_H 2} + \left(\frac{\partial w}{\partial \theta_{H^*}}\right)_{\phi^*, c^*_{H^+}, c^*_H 2}\frac{\widetilde{\theta}_{H^*}}{\widetilde{\phi}} + \left(\frac{\partial w}{\partial c_{H^+}}\right)_{\phi^*, \theta^*_{H^*}, c^*_H 2}\frac{\widetilde{c}_{H^+}}{\widetilde{\phi}} + \left(\frac{\partial w}{\partial c_{H_2}}\right)_{\phi^*, \theta^*_{H^*} c^*_{H^+}}\frac{\widetilde{c}_{H_2}}{\widetilde{\phi}} \tag{b.4.28}$$

$$D_{H_2}\sqrt{\frac{j\omega}{D_{H_2}}}\,\frac{\widetilde{c}_{H_2}}{\widetilde{\phi}} = \left(\frac{\partial r_2}{\partial \phi}\right)_{\theta^*_{H^*}, c^*_{H^+}, c^*_H 2} + \left(\frac{\partial r_2}{\partial \theta_{H^*}}\right)_{\phi^*, c^*_{H^+}, c^*_H 2}\frac{\widetilde{\theta}_{H^*}}{\widetilde{\phi}} + \left(\frac{\partial r_2}{\partial c_{H^+}}\right)_{\phi^*, \theta^*_{H^*}, c^*_H 2}\frac{\widetilde{c}_{H^+}}{\widetilde{\phi}} + \left(\frac{\partial r_2}{\partial c_{H_2}}\right)_{\phi^*, \theta^*_{H^*}, c^*_{H^+}}\frac{\widetilde{c}_{H_2}}{\widetilde{\phi}} \tag{b.4.29}$$

Similar to the previous diffusion-free model, we can define the function $g = \frac{d\theta_H}{dt}$. This time $g = g(\phi, \theta_{H^*}, c_{H^+}, c_{H_2})$.

$$j\omega\frac{\widetilde{\theta}_{H^*}}{\widetilde{\phi}} = \left(\frac{\partial g}{\partial \phi}\right)_{\theta^*_{H^*}, c^*_{H^+}, c^*_{H_2}} + \left(\frac{\partial g}{\partial \theta_{H^*}}\right)_{\phi^*, c^*_{H^+}, c^*_{H_2}}\frac{\widetilde{\theta}_{H^*}}{\widetilde{\phi}} + \left(\frac{\partial g}{\partial c_{H^+}}\right)_{\phi^*, \theta^*_{H^*}, c^*_{H_2}}\frac{\widetilde{c}_{H^+}}{\widetilde{\phi}} + \left(\frac{\partial g}{\partial c_{H_2}}\right)_{\phi^*, \theta^*_{H^*}, c^*_{H^+}}\frac{\widetilde{c}_{H_2}}{\widetilde{\phi}} \tag{b.4.30}$$

Solving the system of equations made by (b.4.28), (b.4.29) and (b.4.30), it is possible to find the expression of the three unknown terms $\frac{\widetilde{\theta}_{H^*}}{\widetilde{\phi}}$, $\frac{\widetilde{c}_{H^+}}{\widetilde{\phi}}$ and $\frac{\widetilde{c}_{H_2}}{\widetilde{\phi}}$. Substituting the solutions into (b.4.2), we find the final expression of Faradaic admittance for Volmer-Heyrovsky mechanism with the inclusion of diffusion correction.

B.5. 1D diffusion corrected molecular hydrogen volmer-heyrovsky model

In this case, in contrast to the previous one, the Faradaic current density is dependent by polarization potential, H* and H_2* coverages and just H^+ concentration at electrode surface:

$$i_F = i_F\left(\phi, \theta_{H^*}, \theta_{H_2^*}, c_{H^+}\right) \tag{b.5.1}$$

The first order Taylor series expansion applied to (b.5.1) brings to the expression of Faradaic admittance.

$$\frac{1}{Z_F} = \left(\frac{\partial i_F}{\partial \phi}\right)_{\theta^*_{H^*}, \theta^*_{H_2^*} c^*_{H^+}} + \left(\frac{\partial i_F}{\partial \theta_{H^*}}\right)_{\phi^*, \theta^*_{H_2^*}, c^*_{H^+}}\frac{\widetilde{\theta}_{H^*}}{\widetilde{\phi}} + \left(\frac{\partial i_F}{\partial \theta_{H_2^*}}\right)_{\phi^*, \theta^*_{H^*} c^*_{H^+}}\frac{\widetilde{\theta}_{H_2^*}}{\widetilde{\phi}} + \left(\frac{\partial i_F}{\partial c_{H^+}}\right)_{\phi^*, \theta^*_{H^*}, \theta^*_{H_2^*}}\frac{\widetilde{c}_{H^+}}{\widetilde{\phi}} \tag{b.5.2}$$

The set of equations (b.4.10)-(b.4.13) and solutions (b.4.14)-(b.4.15) still describes correctly the behavior of H^+ and H_2 concentration at electrode surface for molecular hydrogen Volmer-Heyrovsky. But we should change the boundary conditions. For H^+:

$$If\ x = \infty:\ \Delta c_{H^+}(x,\omega) = 0 \tag{b.5.3}$$

$$If\ x = 0:\ \Delta J_{H^+}(x,\omega) = \Delta(-r_1 - r_2) \tag{b.5.4}$$

And for H_2:

$$If\ x = \infty:\ \Delta c_{H_2}(x,\omega) = 0 \tag{b.5.5}$$

$$If\ x = 0:\ \Delta J_{H_2}(x,\omega) = \Delta r_3 \tag{b.5.6}$$

From (b.5.3) and (b.5.4) we obtain:

$$\Delta c_{H^+}(x,\omega) = N(\omega)e^{-x\sqrt{\frac{j\omega}{D_{H^+}}}} \tag{b.5.7}$$

$$\Delta(-r_1 - r_2) = D_{H^+}\sqrt{\frac{j\omega}{D_{H^+}}}\Delta c_{H^+}(x,\omega) \tag{b.5.8}$$

And from (b.5.5) and (b.5.6) we obtain:

$$\Delta c_{H_2}(x,\omega) = N(\omega)e^{-x\sqrt{\frac{j\omega}{D_{H_2}}}} \tag{b.5.9}$$

$$\Delta r_3 = D_{H_2}\sqrt{\frac{j\omega}{D_{H_2}}}\Delta c_{H_2}(x,\omega) \tag{b.5.10}$$

Defining $w = -r_1 - r_2$, it is possible to rewrite Δw and Δr_3 with a first order Taylor series expansion. The expression of $r_1\left(\phi,\theta_{H^*},\theta_{H_2^*},c_{H^+}\right)$, $r_2\left(\phi,\theta_{H^*},\theta_{H_2^*},c_{H^+}\right)$ and $r_3\left(\theta_{H^*},\theta_{H_2^*},c_{H_2}\right)$ is defined by (a.2.4), (a.2.5) and (a.2.6) from the microkinetic discussion, respectively.

$$\Delta w = \left(\frac{\partial w}{\partial \phi}\right)_{\theta^*_{H^*},\theta^*_{H_2^*},c^*_{H^+}} + \left(\frac{\partial w}{\partial \theta_{H^*}}\right)_{\phi^*,\theta^*_{H_2^*},c^*_{H^+}}\Delta\theta_{H^*} + \left(\frac{\partial w}{\partial \theta_{H_2^*}}\right)_{\phi^*,\theta^*_{H^*}c^*_{H^+}}\Delta\theta_{H_2^*} + \left(\frac{\partial w}{\partial c_{H^+}}\right)_{\phi^*,\theta^*_{H^*},\theta^*_{H_2^*}}\Delta c_{H^+} \tag{b.5.11}$$

$$\Delta r_3 = \left(\frac{\partial r_3}{\partial \theta_{H^*}}\right)_{\phi^*,\theta^*_{H_2^*},c^*_H 2}\Delta\theta_{H^*} + \left(\frac{\partial r_3}{\partial \theta_{H_2^*}}\right)_{\phi^*,\theta^*_{H^*},c^*_H 2}\Delta\theta_{H_2^*} + \left(\frac{\partial r_3}{\partial c_{H_2}}\right)_{\phi^*,\theta^*_{H^*},\theta^*_{H_2^*}}\Delta c_{H_2} \tag{b.5.12}$$

Substituting (b.5.11) in (b.5.8) and (b.5.12) in (b.5.10), expressing perturbation terms with exponential form, and dividing by $\widetilde{\phi}$, it is possible to write:

$$D_{H^+}\sqrt{\frac{j\omega}{D_{H^+}}}\frac{\widetilde{c}_{H^+}}{\widetilde{\phi}} = \left(\frac{\partial w}{\partial \phi}\right)_{\theta^*_{H^*},\theta^*_{H_2^*},c^*_{H^+}} + \left(\frac{\partial w}{\partial \theta_{H^*}}\right)_{\phi^*,\theta^*_{H_2^*}c^*_{H^+}}\frac{\widetilde{\theta}_{H^*}}{\widetilde{\phi}} + \left(\frac{\partial w}{\partial \theta_{H_2^*}}\right)_{\phi^*,\theta^*_{H^*}c^*_{H^+}}\frac{\widetilde{\theta}_{H_2^*}}{\widetilde{\phi}} + \left(\frac{\partial w}{\partial c_{H^+}}\right)_{\phi^*,\theta^*_{H^*},\theta^*_{H_2^*}}\frac{\widetilde{c}_{H^+}}{\widetilde{\phi}} \tag{b.5.13}$$

$$D_{H_2}\sqrt{\frac{j\omega}{D_{H_2}}}\frac{\widetilde{c}_{H_2}}{\widetilde{\phi}} = \left(\frac{\partial r_3}{\partial \theta_{H^*}}\right)_{\phi^*,\theta^*_{H_2^*},c^*_H 2}\frac{\widetilde{\theta}_{H^*}}{\widetilde{\phi}} + \left(\frac{\partial r_3}{\partial \theta_{H_2^*}}\right)_{\phi^*,\theta^*_{H^*},c^*_H 2}\frac{\widetilde{\theta}_{H_2^*}}{\widetilde{\phi}} + \left(\frac{\partial r_3}{\partial c_{H_2}}\right)_{\phi^*,\theta^*_{H^*}\theta^*_{H_2^*}}\frac{\widetilde{c}_{H_2}}{\widetilde{\phi}} \tag{b.5.14}$$

We can express the functions $g = \frac{d\theta_{H^*}}{dt}$ and $q = \frac{d\theta_{H_2^*}}{dt}$ starting from a first order Taylor series expansion. This time $g = g(\phi,\theta_{H^*},c_{H^+})$ and $q = q\left(\phi,\theta_{H^*},\theta_{H_2^*},c_{H^+},c_{H_2}\right)$.

$$j\omega\frac{\widetilde{\theta}_{H^*}}{\widetilde{\phi}} = \left(\frac{\partial g}{\partial \phi}\right)_{\theta^*_{H^*},c^*_{H^+}} + \left(\frac{\partial g}{\partial \theta_{H^*}}\right)_{\phi^*,c^*_{H^+}}\frac{\widetilde{\theta}_{H^*}}{\widetilde{\phi}} + \left(\frac{\partial g}{\partial c_{H^+}}\right)_{\phi^*,\theta^*_{H^*}}\frac{\widetilde{c}_{H^+}}{\widetilde{\phi}} \tag{b.5.15}$$

$$j\omega\frac{\widetilde{\theta}_{H_2^*}}{\widetilde{\phi}} = \left(\frac{\partial q}{\partial \phi}\right)_{\theta^*_{H^*},\theta^*_{H_2^*},c^*_{H^+},c^*_{H_2}} + \left(\frac{\partial q}{\partial \theta_{H^*}}\right)_{\phi^*,\theta^*_{H_2^*},c^*_{H^+},c^*_{H_2}}\frac{\widetilde{\theta}_{H^*}}{\widetilde{\phi}} + \left(\frac{\partial q}{\partial \theta_{H_2^*}}\right)_{\phi^*,\theta^*_{H^*},c^*_{H^+},c^*_{H_2}}\frac{\widetilde{\theta}_{H_2^*}}{\widetilde{\phi}} + \left(\frac{\partial q}{\partial c_{H^+}}\right)_{\phi^*,\theta^*_{H^*},\theta^*_{H_2^*},c^*_{H_2}}\frac{\widetilde{c}_{H^+}}{\widetilde{\phi}} + \left(\frac{\partial q}{\partial c_{H_2}}\right)_{\phi^*,\theta^*_{H^*}\theta^*_{H_2^*},c^*_{H^+}}\frac{\widetilde{c}_{H_2}}{\widetilde{\phi}} \tag{b.5.16}$$

Solving the system of equations made by (b.5.13), (b.5.14), (b.5.15) and (b.5.16), it is possible to find the expression of the three unknown terms $\frac{\widetilde{\theta}_{H^*}}{\widetilde{\phi}}$, $\frac{\widetilde{\theta}_{H_2^*}}{\widetilde{\phi}}$ and $\frac{\widetilde{c}_{H^+}}{\widetilde{\phi}}$. Substituting the solutions into (b.5.2), we find the final expression of Faradaic admittance for diffusion-corrected Volmer-Heyrovsky mechanism passing through the formation of hydrogen complexes.

B.6. EIS parameters

For Volmer-Heyrovsky mechanism, after substituting Faradaic impedance expression in (2.2.6), it is possible to compare the total electrochemical impedance expression with the following mathematical expression:

$$Z = \frac{a_2 + a_3 x}{a_5 + a_6 x + x^2} \tag{b.6.1}$$

Where $x = j\omega$. We obtain the following parameters:

$$a_2 = -\left(\frac{\partial g}{\partial \theta_{H^*}}\right)_{\phi^*}C_{dl}^{-1} \tag{b.6.2}$$

$$a_3 = C_{dl}^{-1} \tag{b.6.3}$$

$$a_4 = -\left(-\left(\frac{\partial i_F}{\partial \theta_{H^*}}\right)_{\phi^*}\left(\frac{\partial g}{\partial \phi}\right)_{\theta^*_{H^*}} + \left(\frac{\partial i_F}{\partial \phi}\right)_{\theta^*_{H^*}}\left(\frac{\partial g}{\partial \theta_{H^*}}\right)_{\phi^*}\right)C_{dl}^{-1} \tag{b.6.4}$$

$$a_5 = -\left(-\left(\frac{\partial i_F}{\partial \phi}\right)_{\theta^*_{H^*}}C_{dl}^{-1} + \left(\frac{\partial g}{\partial \theta_{H^*}}\right)_{\phi^*}\right) \tag{b.6.5}$$

For molecular hydrogen Volmer-Heyrovsky mechanism, after substituting (b.2.11) into (2.20), the final impedance expression should be compared with the mathematical expression:

$$Z = \frac{a_1 + a_2 x + a_3 x^2}{a_4 + a_5 x + a_6 x^2 + x^3} \tag{b.6.6}$$

We obtain the following parameters:

$$a_1 = -\left(\left(\frac{\partial g}{\partial \theta_{H_2^*}} \right)_{\theta^*_{H^*}, \theta^*_{H_2^*}} \left(\frac{\partial q}{\partial \theta_{H^*}} \right)_{\phi^*, \theta^*_{H_2^*}} - \left(\frac{\partial g}{\partial \theta_{H^*}} \right)_{\phi^*, \theta^*_{H_2^*}} \left(\frac{\partial q}{\partial \theta_{H_2^*}} \right)_{\phi^*, \theta^*_{H^*}} \right) C_{dl}^{-1} \tag{b.6.7}$$

$$a_2 = -\left(\left(\frac{\partial g}{\partial \theta_{H^*}} \right)_{\phi^*, \theta^*_{H_2^*}} + \left(\frac{\partial q}{\partial \theta_{H_2^*}} \right)_{\phi^*, \theta^*_{H^*}} \right) C_{dl}^{-1} \tag{b.6.8}$$

$$a_3 = C_{dl}^{-1} \tag{b.6.9}$$

$$a_4 = -\left(\left(\frac{\partial i_F}{\partial \theta_{H_2^*}} \right)_{\phi^*, \theta^*_{H^*}} \left(\frac{\partial g}{\partial \theta_{H^*}} \right)_{\phi^*, \theta^*_{H_2^*}} \left(\frac{\partial q}{\partial \phi} \right)_{\theta^*_{H^*}, \theta^*_{H_2^*}} - \left(\frac{\partial i_F}{\partial \theta_{H^*}} \right)_{\phi^*, \theta^*_{H_2^*}} \left(\frac{\partial g}{\partial \theta_{H_2^*}} \right)_{\theta^*_{H^*}, \theta^*_{H_2^*}} \left(\frac{\partial q}{\partial \phi} \right)_{\theta^*_{H^*}, \theta^*_{H_2^*}} - \right.$$
$$\left(\frac{\partial i_F}{\partial \theta_{H_2^*}} \right)_{\phi^*, \theta^*_{H^*}} \left(\frac{\partial g}{\partial \phi} \right)_{\theta^*_{H^*}, \theta^*_{H_2^*}} \left(\frac{\partial q}{\partial \theta_{H^*}} \right)_{\phi^*, \theta^*_{H_2^*}} + \left(\frac{\partial i_F}{\partial \phi} \right)_{\theta^*_{H^*}, \theta^*_{H_2^*}} \left(\frac{\partial g}{\partial \theta_{H_2^*}} \right)_{\theta^*_{H^*}, \theta^*_{H_2^*}} \left(\frac{\partial q}{\partial \theta_{H^*}} \right)_{\phi^*, \theta^*_{H_2^*}} + \tag{b.6.10}$$
$$\left. \left(\frac{\partial i_F}{\partial \theta_{H^*}} \right)_{\phi^*, \theta^*_{H_2^*}} \left(\frac{\partial g}{\partial \phi} \right)_{\theta^*_{H^*}, \theta^*_{H_2^*}} \left(\frac{\partial q}{\partial \theta_{H_2^*}} \right)_{\phi^*, \theta^*_{H^*}} - \left(\frac{\partial i_F}{\partial \phi} \right)_{\theta^*_{H^*}, \theta^*_{H_2^*}} \left(\frac{\partial g}{\partial \theta_{H^*}} \right)_{\phi^*, \theta^*_{H_2^*}} \left(\frac{\partial q}{\partial \theta_{H_2^*}} \right)_{\phi^*, \theta^*_{H^*}} \right) C_{dl}^{-1}$$

$$a_5 = -\left(- \left(\frac{\partial i_F}{\partial \theta_{H^*}} \right)_{\phi^*, \theta^*_{H_2^*}} \left(\frac{\partial g}{\partial \phi} \right)_{\theta^*_{H^*}, \theta^*_{H_2^*}} + \left(\frac{\partial i_F}{\partial \phi} \right)_{\theta^*_{H^*}, \theta^*_{H_2^*}} \left(\frac{\partial g}{\partial \theta_{H^*}} \right)_{\phi^*, \theta^*_{H_2^*}} - \left(\frac{\partial i_F}{\partial \theta_{H_2^*}} \right)_{\phi^*, \theta^*_{H^*}} \left(\frac{\partial q}{\partial \phi} \right)_{\theta^*_{H^*}, \theta^*_{H_2^*}} + C_{dl} \left(\frac{\partial g}{\partial \theta_{H_2^*}} \right)_{\theta^*_{H^*}, \theta^*_{H_2^*}} \left(\frac{\partial q}{\partial \theta_{H^*}} \right)_{\phi^*, \theta^*_{H_2^*}} + \left(\frac{\partial q}{\partial \theta_{H_2^*}} \right)_{\phi^*, \theta^*_{H^*}} \left(\frac{\partial i_F}{\partial \phi} \right)_{\theta^*_{H^*}, \theta^*_{H_2^*}} \right.$$
$$\left. - C_{dl} \left(\frac{\partial q}{\partial \theta_{H_2^*}} \right)_{\phi^*, \theta^*_{H^*}} \left(\frac{\partial g}{\partial \theta_{H^*}} \right)_{\phi^*, \theta^*_{H_2^*}} \right) C_{dl}^{-1} \tag{b.6.11}$$

$$a_6 = -\left(- \left(\frac{\partial i_F}{\partial \phi} \right)_{\theta^*_{H^*}, \theta^*_{H_2^*}} + C_{dl} \left(\frac{\partial g}{\partial \theta_{H^*}} \right)_{\phi^*, \theta^*_{H_2^*}} + C_{dl} \left(\frac{\partial q}{\partial \theta_{H_2^*}} \right)_{\phi^*, \theta^*_{H^*}} \right) C_{dl}^{-1} \tag{b.6.12}$$

Data availability

Data will be made available on request.

References

[1] G. Centi, J. Čejka, Needs and gaps for catalysis in addressing transitions in chemistry and energy from a sustainability perspective, ChemSusChem 12 (2019) 621–632, https://doi.org/10.1002/cssc.201802637.

[2] M. Capdevila-Cortada, Electrifying the haber–bosch, Nat. Catal. 2 (2019) 1055, https://doi.org/10.1038/s41929-019-0414-4. –1055.

[3] W.A. Smith, T. Burdyny, D.A. Vermaas, H. Geerlings, Pathways to industrial-scale fuel out of thin air from CO2 electrolysis, Joule 3 (2019) 1822–1834, https://doi.org/10.1016/j.joule.2019.07.009.

[4] J.T. Bender, A.S. Petersen, F.C. Østergaard, M.A. Wood, S.M.J. Heffernan, D. J. Milliron, J. Rossmeisl, J. Resasco, Understanding cation effects on the hydrogen evolution reaction, ACS Energy Lett. 8 (2023) 657–665, https://doi.org/10.1021/acsenergylett.2c02500.

[5] D. Strmcnik, P.P. Lopes, B. Genorio, V.R. Stamenkovic, N.M. Markovic, Design principles for hydrogen evolution reaction catalyst materials, Nano Energy 29 (2016) 29–36, https://doi.org/10.1016/j.nanoen.2016.04.017.

[6] X. Zou, Y. Zhang, Noble metal-free hydrogen evolution catalysts for water splitting, Chem. Soc. Rev. 44 (2015) 5148–5180, https://doi.org/10.1039/c4cs00448e.

[7] J.D. Benck, T.R. Hellstern, J. Kibsgaard, P. Chakthranont, T.F. Jaramillo, Catalyzing the hydrogen evolution reaction (HER) with molybdenum sulfide nanomaterials, ACS Catal. 4 (2014) 3957–3971, https://doi.org/10.1021/cs500923c.

[8] Y. Cao, Roadmap and direction toward high-performance MoS $_2$ hydrogen evolution catalysts, ACS Nano 15 (2021) 11014–11039, https://doi.org/10.1021/acsnano.1c01879.

[9] W. Zhou, J. Jia, J. Lu, L. Yang, D. Hou, G. Li, S. Chen, Recent developments of carbon-based electrocatalysts for hydrogen evolution reaction, Nano Energy 28 (2016) 29–43, https://doi.org/10.1016/j.nanoen.2016.08.027.

[10] W. Moschkowitsch, O. Lori, L. Elbaz, Recent progress and viability of PGM-free catalysts for hydrogen evolution reaction and hydrogen oxidation reaction, ACS Catal. 12 (2022) 1082–1089, https://doi.org/10.1021/acscatal.1c04948.

[11] A. Wang, J. Li, T. Zhang, Heterogeneous single-atom catalysis, Nat. Rev. Chem. 2 (2018) 65–81, https://doi.org/10.1038/s41570-018-0010-1.

[12] F. Kraushofer, G.S. Parkinson, Single-atom catalysis: insights from Model Systems, Chem. Rev. 122 (2022) 14911–14939, https://doi.org/10.1021/acs.chemrev.2c00259.

[13] S.K. Kaiser, Z. Chen, D. Faust Akl, S. Mitchell, J. Pérez-Ramírez, Single-atom catalysts across the periodic table, Chem. Rev. 120 (2020) 11703–11809, https://doi.org/10.1021/acs.chemrev.0c00576.

[14] B. Singh, M.B. Gawande, A.D. Kute, R.S. Varma, P. Fornasiero, P. McNeice, R. V. Jagadeesh, M. Beller, R. Zbořil, Single-atom (Iron-Based) catalysts: synthesis and applications, Chem. Rev. 121 (2021) 13620–13697, https://doi.org/10.1021/acs.chemrev.1c00158.

[15] X.F. Yang, A. Wang, B. Qiao, J. Li, J. Liu, T. Zhang, Single-atom catalysts: a new frontier in heterogeneous catalysis, Acc. Chem. Res. 46 (2013) 1740–1748, https://doi.org/10.1021/ar300361m.

[16] C. Copéret, M. Chabanas, R.P. Saint-Arroman, J.-M. Basset, Homogeneous and heterogeneous catalysis: bridging the gap through surface organometallic chemistry, Angew. Chem. Int. Ed. 42 (2003) 156–181, https://doi.org/10.1002/anie.200390072.

[17] Z. Chen, E. Vorobyeva, S. Mitchell, E. Fako, M.A. Ortuño, N. López, S.M. Collins, P. A. Midgley, S. Richard, G. Vilé, J. Pérez-Ramírez, A heterogeneous single-atom

palladium catalyst surpassing homogeneous systems for Suzuki coupling, Nat. Nanotechnol. 13 (2018) 702–707, https://doi.org/10.1038/s41565-018-0167-2.
[18] X. Cui, W. Li, P. Ryabchuk, K. Junge, M. Beller, Bridging homogeneous and heterogeneous catalysis by heterogeneous single-metal-site catalysts, Nat. Catal. 1 (2018) 385–397, https://doi.org/10.1038/s41929-018-0090-9.
[19] I. Barlocco, G. Di Liberto, G. Pacchioni, Hydrogen complexes on single atom alloys: classical chemisorption versus coordination chemistry, Catal. Sci. Technol. 13 (2023) 5301–5312, https://doi.org/10.1039/D3CY00609C.
[20] G. Di Liberto, L.A. Cipriano, G. Pacchioni, Role of dihydride and dihydrogen complexes in hydrogen evolution reaction on single-atom catalysts, J. Am. Chem. Soc. 143 (2021) 20431–20441, https://doi.org/10.1021/jacs.1c10470.
[21] J. Lu, P. Serna, B.C. Gates, Zeolite- and MgO-supported molecular iridium complexes: support and ligand effects in catalysis of ethene hydrogenation and H–D exchange in the conversion of $H_2 + D_2$, ACS. Catal. 1 (2011) 1549–1561, https://doi.org/10.1021/cs200397r.
[22] G. Di Liberto, G. Pacchioni, Modeling single-atom catalysis, Adv. Mater. (2023), https://doi.org/10.1002/adma.202307150.
[23] C. Saetta, I. Barlocco, G. Di Liberto, G. Pacchioni, Key ingredients for the screening of single atom catalysts for the hydrogen evolution reaction: the case of titanium nitride, Small 20 (2024), https://doi.org/10.1002/smll.202401058.
[24] S. Ye, F. Liu, F. She, J. Chen, D. Zhang, A. Kumatani, H. Shiku, L. Wei, H. Li, Hydrogen binding energy is insufficient for describing Hydrogen evolution on single-atom catalysts, Angew. Chem. 137 (2025), https://doi.org/10.1002/ange.202425402.
[25] J.T. Mefford, Z. Zhao, M. Bajdich, W.C. Chueh, Interpreting Tafel behavior of consecutive electrochemical reactions through combined thermodynamic and steady state microkinetic approaches, Energy Env. Sci. 13 (2020) 622–634, https://doi.org/10.1039/C9EE02697E.
[26] C.F. Dickens, C. Kirk, J.K. Nørskov, Insights into the electrochemical oxygen evolution reaction with ab initio calculations and microkinetic modeling: beyond the limiting potential volcano, J. Phys. Chem. C 123 (2019) 18960–18977, https://doi.org/10.1021/acs.jpcc.9b03830.
[27] H. Feng, M. Zhang, Z. Ge, Y. Deng, P. Pu, W. Zhou, H. Yuan, J. Yang, F. Li, X. Zhang, Y.W. Zhang, Designing efficient single-atom alloy catalysts for selective C=O hydrogenation: a first-principles, active learning and microkinetic study, ACS. Appl. Mater. Interfaces. 15 (2023) 55903–55915, https://doi.org/10.1021/acsami.3c15108.
[28] M. Rebarchik, S. Bhandari, T. Kropp, M. Mavrikakis, Insights into the oxygen evolution reaction on graphene-based single-atom catalysts from First-principles-informed microkinetic modeling, ACS. Catal. 13 (2023) 5225–5235, https://doi.org/10.1021/acscatal.3c00474.
[29] D.D. Macdonald, Reflections on the history of electrochemical impedance spectroscopy, Electrochim. Acta 51 (2006) 1376–1388, https://doi.org/10.1016/j.electacta.2005.02.107.
[30] A. Lasia, Mechanism and kinetics of the hydrogen evolution reaction, Int. J. Hydrog. Energy 44 (2019) 19484–19518, https://doi.org/10.1016/j.ijhydene.2019.05.183.
[31] G.B. Kauffman, Electrochemical impedance spectroscopy. by mark E. orazem and bernard tribollet, Angew. Chem. Int. Ed. 48 (2009), https://doi.org/10.1002/anie.200805564.
[32] E.B. Castro, M.J. De Giz, E.R. Gonzalez2, J.R. Vilche', An electrochemical impedance study on the kinetics and mechanism of the hydrogen evolution reaction on nickel molybdenite electrodes, 1997.
[33] A. Lasia, Study of electrode activities towards the hydrogen evolution reaction by a.C. impedance spectroscopy, 1993.
[34] V.I. Kichigin, A.B. Shein, Diagnostic criteria for hydrogen evolution mechanisms in electrochemical impedance spectroscopy, Electrochim. Acta 138 (2014) 325–333, https://doi.org/10.1016/j.electacta.2014.06.114.
[35] R. Garcia-Garcia, J.G. Rivera, R. Antaño-Lopez, F. Castañeda-Olivares, G. Orozco, Impedance spectra of the cathodic hydrogen evolution reaction on polycrystalline rhenium, Int. J. Hydrog. Energy 41 (2016) 4660–4669, https://doi.org/10.1016/j.ijhydene.2016.01.010.
[36] D.A. Harrington, B.E. Conway, Ac impedance of faradaic reactions involving electrosorbed intermediates-I. Kinet Theory, n.d.
[37] D. Koster, A.R. Zeradjanin, A. Battistel, F.La Mantia, Extracting the kinetic parameters of the hydrogen evolution reaction at Pt in acidic media by means of dynamic multi-frequency analysis, Electrochim. Acta 308 (2019), https://doi.org/10.1016/j.electacta.2019.04.013.
[38] N. Pianta, F. Scarpioni, R. Chukwu, F. La Mantia, R. Ruffo, Evaluation of kinetic parameters of non-faradic processes in carbon-based electrodes using multisine dynamic electrochemical impedance spectroscopy, Electrochim. Acta 437 (2023) 141462, https://doi.org/10.1016/j.electacta.2022.141462.
[39] F. Scarpioni, S. Khalid, R. Chukwu, N. Pianta, F. La Mantia, R. Ruffo, Electrochemical impedance spectroscopy for electrode process evaluation: lithium titanium phosphate in concentrated aqueous electrolyte, ChemElectroChem 10 (2023), https://doi.org/10.1002/celc.202201133.
[40] D. Koster, G. Du, A. Battistel, F.La Mantia, Dynamic impedance spectroscopy using dynamic multi-frequency analysis: a theoretical and experimental investigation, Electrochim. Acta 246 (2017) 553–563, https://doi.org/10.1016/j.electacta.2017.06.060.
[41] N. Hallemans, D. Howey, A. Battistel, N.F. Saniee, F. Scarpioni, B. Wouters, F. La Mantia, A. Hubin, W.D. Widanage, J. Lataire, Electrochemical impedance spectroscopy beyond linearity and stationarity—A critical review, Electrochim. Acta 466 (2023), https://doi.org/10.1016/j.electacta.2023.142939.
[42] C. Saetta, G. Di Liberto, G. Pacchioni, Water splitting on a Pt1/C3N4 single atom catalyst: a modeling approach, Top. Catal. (2023), https://doi.org/10.1007/s11244-023-01802-x.
[43] M. Spotti, G. Di Liberto, G. Pacchioni, CO2 Activation on single-atom catalysts: importance of the supporting matrix, Top. Catal. (2025), https://doi.org/10.1007/s11244-025-02064-5.
[44] M.M.O. Thotiyl, T.R. Kumar, S. Sampath, Pd supported on titanium nitride for efficient ethanol oxidation, J. Phys. Chem. C 114 (2010) 17934–17941, https://doi.org/10.1021/jp1038514.
[45] S. Yang, J. Kim, Y.J. Tak, A. Soon, H. Lee, Single-atom catalyst of platinum supported on titanium nitride for selective electrochemical reactions, Angew. Chem. Int. Ed. 55 (2016) 2058–2062, https://doi.org/10.1002/anie.201509241.
[46] M. Umer, S. Umer, M. Zafari, M. Ha, R. Anand, A. Hajibabaei, A. Abbas, G. Lee, K. S. Kim, Machine learning assisted high-throughput screening of transition metal single atom based superb hydrogen evolution electrocatalysts, J. Mater. Chem. Mater. 10 (2022) 6679–6689, https://doi.org/10.1039/D1TA09878K.
[47] A. Bagger, W. Ju, A.S. Varela, P. Strasser, J. Rossmeisl, Single site porphyrine-like structures advantages over metals for selective electrochemical CO2 reduction, Catal. Today 288 (2017) 74–78, https://doi.org/10.1016/j.cattod.2017.02.028.
[48] A.J. Bard, L.R. Faulkner, H.S. White, Electrochemical methods : Fundamentals and Applications, John Wiley & Sons, Ltd., 2022.
[49] M.C.O. Monteiro, F. Dattila, N. López, M.T.M. Koper, The role of cation acidity on the competition between hydrogen evolution and CO_2 reduction on gold electrodes, J. Am. Chem. Soc. 144 (2022) 1589–1602, https://doi.org/10.1021/jacs.1c10171.
[50] M.C.O. Monteiro, F. Dattila, B. Hagedoorn, R. García-Muelas, N. López, M.T. M. Koper, Absence of CO2 electroreduction on copper, gold and silver electrodes without metal cations in solution, Nat. Catal. 4 (2021) 654–662, https://doi.org/10.1038/s41929-021-00655-5.
[51] J.T. Bender, A.S. Petersen, F.C. Østergaard, M.A. Wood, S.M.J. Heffernan, D. J. Milliron, J. Rossmeisl, J. Resasco, Understanding cation effects on the hydrogen evolution reaction, ACS Energy Lett. 8 (2023) 657–665, https://doi.org/10.1021/acsenergylett.2c02500.
[52] M. Muhyuddin, N. Pianta, J.A. Trindell, R. Ruffo, C. Santoro, M.T. Koper, Cation effects on the hydrogen evolution reaction by catalysts based on cobalt complexes in alkaline electrolytes, Electrochim. Acta 535 (2025) 146684, https://doi.org/10.1016/j.electacta.2025.146684.
[53] A. Goyal, M.T.M. Koper, The interrelated effect of cations and electrolyte pH on the hydrogen evolution reaction on gold electrodes in alkaline media, Angew. Chem. Int. Ed. 60 (2021) 13452–13462, https://doi.org/10.1002/anie.202102803.
[54] G. Kresse, J. Hafner, Ab initio molecular dynamics for liquid metals, Phys. Rev. B 47 (1993) 558–561, https://doi.org/10.1103/PhysRevB.47.558.
[55] G. Kresse, J. Furthmüller, Efficiency of ab-initio total energy calculations for metals and semiconductors using a plane-wave basis set, Comput. Mater. Sci. 6 (1996) 15–50, https://doi.org/10.1016/0927-0256(96)00008-0.
[56] G. Kresse, J. Furthmüller, Efficient iterative schemes for ab initio total-energy calculations using a plane-wave basis set, Phys. Rev. B 54 (1996) 11169–11186, https://doi.org/10.1103/PhysRevB.54.11169.
[57] J.P. Perdew, K. Burke, M. Ernzerhof, Generalized gradient approximation made simple, Phys. Rev. Lett. 77 (1996) 3865–3868, https://doi.org/10.1103/PhysRevLett.77.3865.
[58] P.E. Blöchl, Projector augmented-wave method, Phys. Rev. B 50 (1994) 17953–17979, https://doi.org/10.1103/PhysRevB.50.17953.
[59] G. Kresse, D. Joubert, From ultrasoft pseudopotentials to the projector augmented-wave method, Phys. Rev. B 59 (1999) 1758–1775, https://doi.org/10.1103/PhysRevB.59.1758.
[60] G. Di Liberto, L.A. Cipriano, G. Pacchioni, Universal principles for the rational design of single atom electrocatalysts? Handle with care, ACS. Catal. (2022) 5846–5856, https://doi.org/10.1021/acscatal.2c01011.
[61] I. Barlocco, L.A. Cipriano, G. Di Liberto, G. Pacchioni, Modeling hydrogen and oxygen evolution reactions on single atom catalysts with density functional theory: role of the functional, Adv. Theory Simul. (2022) 2200513, https://doi.org/10.1002/adts.202200513.
[62] I.V. Solovyev, P.H. Dederichs, V.I. Anisimov, Corrected atomic limit in the local-density approximation and the electronic structure of d impurities in Rb, Phys. Rev. B 50 (1994) 16861–16871, https://doi.org/10.1103/PhysRevB.50.16861.
[63] S. Grimme, J. Antony, S. Ehrlich, H. Krieg, A consistent and accurate ab initio parametrization of density functional dispersion correction (DFT-D) for the 94 elements H-Pu, J. Chem. Phys. 132 (2010) 154104, https://doi.org/10.1063/1.3382344.
[64] J.K. Nørskov, T. Bligaard, A. Logadottir, J.R. Kitchin, J.G. Chen, S. Pandelov, U. Stimming, Trends in the exchange current for hydrogen evolution, J. Electrochem. Soc. 152 (2005) J23, https://doi.org/10.1149/1.1856988.
[65] J.K. Nørskov, J. Rossmeisl, A. Logadottir, L. Lindqvist, J.R. Kitchin, T. Bligaard, H. Jónsson, Origin of the overpotential for oxygen reduction at a fuel-cell cathode, J. Phys. Chem. B 108 (2004) 17886–17892, https://doi.org/10.1021/jp047349j.
[66] J.K. Nørskov, T. Bligaard, J. Rossmeisl, C.H. Christensen, Towards the computational design of solid catalysts, Nat. Chem. 1 (2009) 37–46, https://doi.org/10.1038/nchem.121.
[67] J.K. Nørskov, T. Bligaard, A. Logadottir, J.R. Kitchin, J.G. Chen, S. Pandelov, U. Stimming, Trends in the exchange current for hydrogen evolution, J. Electrochem. Soc. 152 (2005) J23, https://doi.org/10.1149/1.1856988.
[68] K.S. Exner, H. Over, Kinetics of electrocatalytic reactions from first-principles: a critical comparison with the ab initio thermodynamics approach, Acc. Chem. Res. 50 (2017) 1240–1247, https://doi.org/10.1021/acs.accounts.7b00077.

[69] B.J. O, M. Bockris, I.A. Ammar, A.K.M S Huq, A. Steinberg, S.S. Carlton, E. Sibcrt, E. Yeager, T.S. Oey, F. Hovorka, Hydrogen evolution reaction on Pt, Ag and W surfaces in acids the mechanism of the hydrogen evolution reaction on platinum silver and tungsten surfaces in acid solutions relatively thick Pt wires do not make a tight seal with hysil in Hs but do in Os, UTC. https://pubs.acs.org/sharingguidelines, 1955.
[70] Y. Huang, R.J. Nielsen, W.A. Goddard, Reaction mechanism for the hydrogen evolution Reaction on the basal plane sulfur vacancy site of MoS 2 using grand canonical potential kinetics, J. Am. Chem. Soc. 140 (2018) 16773–16782, https://doi.org/10.1021/jacs.8b10016.
[71] S. Osella, W.A. Goddard, CO2 Reduction to methane and ethylene on a single-atom catalyst: a grand canonical Quantum Mechanics study, J. Am. Chem. Soc. 145 (2023) 21319–21329, https://doi.org/10.1021/jacs.3c05650.
[72] G.J. Kubas, Molecular hydrogen complexes: coordination of a .sigma. Bond to transition metals, Acc. Chem. Res. 21 (1988) 120–128, https://doi.org/10.1021/ar00147a005.
[73] G.J. Kubas, Fundamentals of H 2 binding and reactivity on transition metals underlying hydrogenase function and H 2 production and storage, Chem. Rev. 107 (2007) 4152–4205, https://doi.org/10.1021/cr050197j.
[74] D.M. Heinekey, A. Lledós, J.M. Lluch, Elongated dihydrogen complexes: what remains of the H–H Bond? Chem. Soc. Rev. 33 (2004) 175–182, https://doi.org/10.1039/B304879A.
[75] T. Shinagawa, A.T. Garcia-Esparza, K. Takanabe, Insight on Tafel slopes from a microkinetic analysis of aqueous electrocatalysis for energy conversion, Sci. Rep. 5 (2015) 13801, https://doi.org/10.1038/srep13801.
[76] A. Lasia, Mechanism and kinetics of the hydrogen evolution reaction, Int. J. Hydrog. Energy 44 (2019) 19484–19518, https://doi.org/10.1016/j.ijhydene.2019.05.183.
[77] S. Gautier, S.N. Steinmann, C. Michel, P. Fleurat-Lessard, P. Sautet, Molecular adsorption at Pt(111). How accurate are DFT functionals? Phys. Chem. Chem. Phys. 17 (2015) 28921–28930, https://doi.org/10.1039/c5cp04534g.
[78] S.M. Sharada, R.K.B. Karlsson, Y. Maimaiti, J. Voss, T. Bligaard, Adsorption on transition metal surfaces: transferability and accuracy of DFT using the ADS41 dataset, Phys. Rev. B 100 (2019), https://doi.org/10.1103/PhysRevB.100.035439.
[79] T.T. Yang, R.B. Patil, J.R. McKone, W.A. Saidi, Revisiting trends in the exchange current for hydrogen evolution, Catal. Sci. Technol. 11 (2021) 6832–6838, https://doi.org/10.1039/d1cy01170g.
[80] S. Anantharaj, S. Noda, How properly are we interpreting the Tafel lines in energy conversion electrocatalysis? Mater. Today Energy 29 (2022) 101123 https://doi.org/10.1016/j.mtener.2022.101123.
[81] M.E. Orazem, P. Aganval ', L.H. Garcia-Rubio ', Critical issues associated with interpretation of impedance spectra l, J. Electroanal. Chem 378 (1994) 51–62.
[82] J. Huang, Z. Li, B.Y. Liaw, J. Zhang, Graphical analysis of electrochemical impedance spectroscopy data in bode and Nyquist representations, J. Power. Sources. 309 (2016) 82–98, https://doi.org/10.1016/j.jpowsour.2016.01.073.
[83] P. Ekdunge, K. Jüttner, G. Kreysa, T. Kessler, M. Ebert, W.J. Lorenz, Electrochemical impedance study on the kinetics of hydrogen evolution at amorphous metals in alkaline solution, J. Electrochem. Soc. 138 (1991) 2660–2668, https://doi.org/10.1149/1.2086034.
[84] A. Bowden, A. Reports, General equations for the kinetics of electrode processes, 1938.
[85] E. Van Gheem, E. Tourwé, R. Pintelon, A. Hubin, A theoretical approach for modelling electrochemical impedance measurements using a rational function in jω, J. Electroanal. Chem. 613 (2008) https://doi.org/10.1016/j.jelechem.2007.10.020.
[86] W. Li, Q.A. Huang, Y. Bai, J. Wang, L. Wang, Y. Liu, Y. Zhao, X. Li, J. Zhang, Model reduction of fractional impedance spectra for time–frequency analysis of batteries, fuel cells, and supercapacitors, Carbon Energy 6 (2024), https://doi.org/10.1002/cey2.360.
[87] J. Huang, Diffusion impedance of electroactive materials, electrolytic solutions and porous electrodes: warburg impedance and beyond, Electrochim. Acta 281 (2018) 170–188, https://doi.org/10.1016/j.electacta.2018.05.136.